

Composite calcite and opal test in Foraminifera (Rhizaria)

Julien Richirt¹, Satoshi Okada¹, Yoshiyuki Ishitani¹, Katsuyuki Uematsu², Akihiro Tame², Kaya Oda¹, Noriyuki Isobe³, Toyoho Ishimura⁴, Masashi Tsuchiya⁵, Hidetaka Nomaki¹

¹ SUGAR, X-star, Japan Agency for Marine-Earth Science and Technology (JAMSTEC), 2-15 Natsushima-cho, Yokosuka 237-0061, Japan

² Marine Works Japan Ltd., 3-54-1 Oppamahigashi-cho, Yokosuka, Kanagawa, 237-0063, Japan

³ Research Institute for Marine Resources Utilization (MRU), Japan Agency for Marine-Earth Science and Technology (JAMSTEC), Yokosuka, Kanagawa, 237-0061, Japan

⁴ Graduate School of Human and Environmental Studies, Kyoto University, Yoshidanihonmatsu, Sakyo-ku, Kyoto 606-8501, Japan

⁵ Research Institute for Global Change (RIGC), Japan Agency for Marine-Earth Science and Technology (JAMSTEC), Yokosuka, Kanagawa, 237-0061, Japan

Correspondence to: Julien Richirt (richirt.julien@gmail.com)

Abstract. Foraminifera are unicellular eukaryotes known to have a shell, called test, generally made of secreted calcite (CaCO₃). We report for the first time a Foraminifera having a composite calcite/opal test in the cosmopolitan and well-studied benthic species *Bolivina spissa* (Rotaliida), sampled from the Sagami Bay in Japan at 1410 m depth. Based on comprehensive investigations including Scanning Electron Microscopy (SEM) coupled with Energy Dispersive X-ray Spectroscopy (EDS) and Fourier Transform Infrared Spectroscopy (FTIR), we inspect the morphology and composition of the novel opaline layer coating the inside part of the calcitic test. Using Scanning Transmission Electron Microscopy (STEM) and EDS analyses, we detected probable Silica Deposition Vesicles (SDVs), organelles involved in opal precipitation in other silicifying organisms, confirming that the Foraminifera themselves secrete the opal layer. The layer was systematically found in all studied individuals and had no apparent sub-structure. Its thickness showed an analogous growth pattern with to the calcitic shell of *B. spissa*, being the thickest in the oldest chamber (proloculus) and becoming thinner toward the younger chambers (apertural side). Its absence in the youngest chambers indicates that silicification occurs subsequently to calcification, probably discontinuously. We further discuss the potential function(s) of this composite test and propose that the opal layer may serve as a protection barrier against predators using either mechanical drilling or chemical etching of the calcitic test. Isotopic composition measurements performed separately on the proloculus part and the apertural side of *B. spissa* suggest that the presence of an opal layer may alter the calcitic isotopic signal and impact paleoenvironmental proxy using foraminifer's tests composition. If silicification in Foraminifera was found to be more widespread than previously thought, it could possibly have important implications for foraminiferal evolution, palaeoceanographic reconstructions, and the silica cycle at global scale.

1 Introduction

Silicon (Si) is the second most abundant element (27.2 wt. %) in the earth crust after oxygen (Greenwood and Earnshaw, 1997). In nature, ~~silicon-Si~~ occurs generally in the form of silicate minerals (e.g., ~~quartz, aluminosilicates,~~ ~~and silicon dioxide~~ (~~SiO₂, e.g., quartz~~). Its soluble form, orthosilicic acid Si(OH)₄, is biologically ~~assimilable~~ ~~available~~, and biogenic silica, also referred to as biogenic opal (amorphous hydrated silica, SiO₂·nH₂O), is the second most abundant mineral type formed by organisms after carbonate minerals. A wide range of marine organisms such as sponges ~~and/or~~ protists, including diatoms, radiolarians ~~and/or~~ silicoflagellates (dictyochales), are able to take up Si(OH)₄ from ~~their~~ surrounding water and use ~~silicon-Si~~ to build their shells or skeletons (Brümmer, 2003; Ehrlich et al., 2016). ~~The~~ ~~s~~ilicified protistan shells ~~were proposed to serve~~ various and not mutually exclusive functions, such as defence against grazers, buoyancy, light modulation, catalysis of carbon assimilation, maintenance of shape and orientation or defence against viruses (Knoll & Kotrc, 2015).

Foraminifera (Rhizaria), belonging to the SAR group (i.e., Stramenopiles, Alveolata and Rhizaria, Burki et al., 2020), are one of the most widespread unicellular eukaryotes inhabiting both benthic and pelagic realms. They are characterised by the presence of a shell, ~~also~~ ~~called~~ a “test”, which can be organic, agglutinated (typically attaching sediment particles) or ~~constituted~~ ~~consist~~ of precipitated minerals, ~~most commonly calcium carbonate (CaCO₃;~~ Sen Gupta, 2003). ~~In the last category, almost all species precipitate calcium carbonate (CaCO₃).~~ Having a high diversity with ~ 4000 recent living hard-shelled species able to fossilise (Murray, 2007), they show a profuse fossil record starting in the Cambrian (Culver, 1991). Consequently, the group is intensively employed for palaeoceanographic studies and palaeoenvironmental reconstructions (e.g., Murray, 2006, Jones, 2013), and geochemical measurements of their tests have been extensively used to gain most of our knowledge on the past ocean responses to climate change (e.g., Katz et al., 2010). Additionally, Foraminifera play an important role in the global carbon cycle through ~~and carbonate production (Langer, 2008) and~~ remineralisation, especially in poorly oxygenated environments (Piña-Ochoa et al., 2010; Cesbron et al., 2016) ~~and carbonate production (Langer, 2008)~~. Although ~~the~~ exact calcification process is still ~~up for~~ ~~in~~ debate (de Nooijer et al., 2014; Toyofuku et al., 2017; Nagai et al., 2018; Ujiie et al., 2023), different foraminiferal sub-orders are known to exhibit different test structure organisations (Hansen, 2003) and geochemical compositions (de Nooijer et al., 2023).

While silica precipitation occurs frequently in most of lineages of the SAR group (Marron et al., 2016), it was only very rarely described in Foraminifera. The first report was made by Brady in ~~the~~ late 19th century, who wrote that the tests of some benthic foraminifera assigned to *Miliolina* from the abyssal ~~area of~~ North Pacific ~~were~~ ~~as~~ not dissolved by acid, and that their usual calcareous shell was totally or partially replaced by a thin siliceous ~~investment~~ ~~external~~ ~~coating~~, which exhibited a perfectly homogeneous texture (p. xvii, Brady, 1884). However, no supplementary information about this observation is available and these specimens might have been agglutinating foraminifera ~~having with~~ a very smooth test. Almost one century later, Echols (1971) reported rare individuals of ‘*Miliolinella*’ sp. presenting a wall insoluble in dilute hydrochloric acid, lacking apparent agglutinated particles, and possibly composed of opaline silica in sediment sampled at various depths (990–4640 m water depth) in the Scotia Sea, Southern Ocean. A benthic foraminiferal species sampled in the Indian Ocean at depths ranging from

5266–5420 m was also described as having an opaline shell, ~~because-as~~ it was insoluble in hydrochloric acid (*Miliammellus* legis, Saidova & Burmistrova, 1978). This species, being the only representative ~~in-of~~ the newly established genus *Miliammellus*, was placed into the order Miliolida because of its general morphology (Burmistrova, 1978). However, Lipps already argued in 1973 that insolubility in acids is not a conclusive experiment, because an organic cement would hold the test together, such as in specimens assigned to Rzehakinidae (Cushman, 1933), introducing foraminifera having a “siliceous or agglutinated” wall that disaggregate in hydrogen peroxide but resist acid dissolution. Additionally, in the case of fossil species that do not disaggregate in hydrogen peroxide, taphonomic processes might have stabilised the organic matter cement, making this test inconclusive for fossilised specimens. In 1980, Resig et al. described a species sampled from the Pacific Ocean at ~4400 m depth as presenting an imperforate test uniquely constituted of silica (*Silicoloculina profunda*, Resig, Lowenstam, Echols & Weiner, 1980), and created a new suborder (*Silicoloculinina*) based on the wall construction type (imperforate test made of secreted opaline silica). The authors imaged the fine structures of the test and investigated its composition, validating its opaline silica nature, and concluding that the test was secreted by the Foraminifera. The remarkable similarity regarding the descriptions given in Burmistrova (1978) and Resig et al. (1980) led to the conclusion that they certainly described the same species, making *Silicoloculina profunda* a junior synonym of *Miliammellus legis* (as referenced in WoRMS database). The presence of silicate grains within the calcitic test was reported in *Melonis baarleanus* (Rotaliida) but were ~~supposed~~ ~~inferred~~ to be ~~from-aof~~ sedimentary origin (Borrelli et al., 2018). While biosilicification ~~has~~ve commonly been reported in other rhizarian groups such as radiolarians ~~and/or~~ cercozoans (Marron et al., 2016; Hendry et al., 2018), only scarce observations of foraminifers having a ~~silica-siliceous~~ test ~~were-have been~~ reported and their silica mineralisation process is totally unknown. To date, *M. legis* (Miliolida) is the only species reported as having a secreted siliceous test for this group.

Here we report the systematic presence of an opaline layer in the test in the cosmopolitan benthic species *Bolivina spissa* (Rotaliida) sampled at 1410 m depth in ~~the~~ Sagami Bay (Japan). The composite test is composed of two different materials: an external calcitic test, typical ~~from-for~~ hyaline and porcelaneous Foraminifera, and an internal layer composed of biogenic silica (opal) coating the inside part of the calcitic test. Different observational and measurement methods were used to describe the composition, morphology and presumed precipitation mechanism of this opal layer, including Scanning Electron Microscopy (SEM), Transmission Electron Microscopy (TEM), Energy-Dispersive X-ray Spectroscopy (EDS) and Fourier-Transform Infrared spectroscopy (FTIR). Based on these comprehensive observations, we ~~further~~-discuss the potential function(s) of this composite test, its potential impact on paleoenvironmental reconstructions using ~~Fforaminifera's~~ tests composition and its possible importance for biogeochemical cycles understanding.

2 Material & Methods

2.1 Sampling sites

Sediment cores were collected using the research deep submergence vehicle (DSV) *Shinkai 6500* on-board R/V *Yokosuka*, in the central part of the Sagami Bay (NSB site, 35°00.3' N 139°22.7' E) at 1410 m depth (Fig. 1), during three sampling campaigns in May 2022 and 2023, and October 2022 (Table 1).

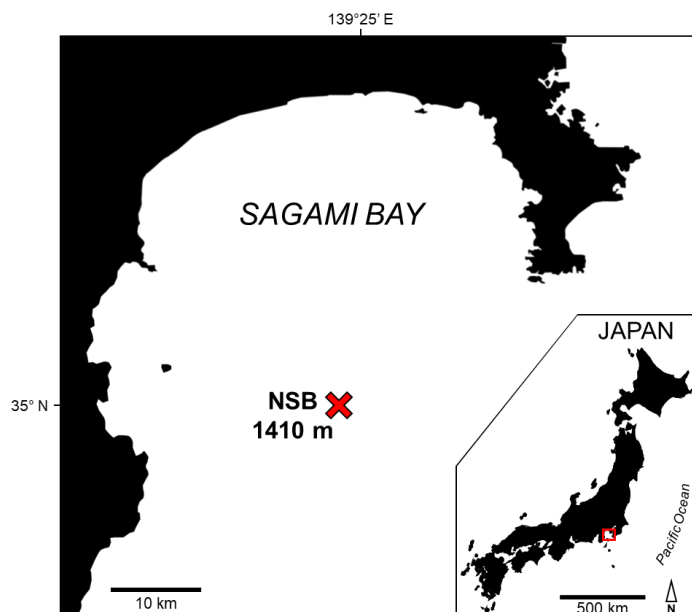


Figure 1: Map of Japan (bottom right panel) indicating the localisation of the Sagami Bay (main panel). Sampling site NSB (red cross) and sampling depth are indicated.

Table 1 summarises the samples origin and the type of analyses performed. *Bolivina spissa* specimens were isolated from different sediment depth intervals (topmost cm or down to 5 cm depth) under a stereomicroscope and were fixed using different techniques (cryo-fixed on board: Okada et al. submitted2024, frozen at -80°C , glutaraldehyde fixed, or air dried).

Table 1: Sampling period, sediment interval, type of analysis, fixation type and timing and number of specimens analysed in this study.

Sampling period	Sediment interval	Type of analyse	Fixation type	Fixation timing	Number of specimens analysed
May 2022	0-1 cm	Cryo-SEM and EDS	Cryo-fixed	Isolated ~1.5 months after sampling from a bucket of sediment stored in the lab at 4°C	1

October 2022	0-1 cm	Cryo-SEM and EDS	Cryo-fixed	Cryo-fixed directly on board after sampling	6
May 2022	0-1 cm and 1-5 cm	Environmental SEM	Frozen at -80°C	Sample frozen -80 °C directly on board after sampling	15
May 2022	every cm from 0-1 cm to 3-4 cm	TEM and EDS	Glutaraldehyde 4%	Fixed directly on board after sampling	8
May 2023	0-2 cm	FTIR spectroscopy	Air dried	Isolated ~3 months after sampling from a bucket of sediment stored in the lab at 4 °C	3
October 2022	0-5 cm	Isotopic composition of calcite	Air-dried	Isolated ~2 months after sampling from a bucket of sediment stored in the lab at 4 °C	17

105 2.2 Cryo-SEM imaging & EDS mapping

After ~~confirming that individuals were live/alive -checks~~ (based on the presence of sediment aggregation at the aperture and cytoplasm coloration), isolated ~~living~~-specimens were processed following the protocol described in Okada et al. (2024submitted). Briefly, specimens were embedded in a sucrose-based or glycerol-based aqueous glue, cryofixed (in liquid nitrogen-cooled isopentane) and stored at c.a. -170 °C. Cross-section of the specimens were exposed using a diamond knife in a cryo-ultramicrotome, aiming for a clean cut to eliminate topographic variations of the sample surface. Scanning electron microscope (SEM) observations ~~were~~ performed on a Helios G4 UX (Thermo Fisher Scientific) equipped with gallium focused ion beam (FIB) gun, an energy dispersive X-ray spectroscopy (EDS) detector (Octane Elite Super C5, AMETEK), and a cryogenic stage with a preparation chamber (PP3010T, Quorum). After sublimation of overlying ~~water-ice crystals~~ (~ 5 min at ~ -80 °C), several SEM images in backscattered electron mode were acquired and aggregated to obtain a high-resolution SEM image for ~~all~~-each individuals (n = 7). The elemental composition was then mapped by EDS analysis without conductive coating of the sample to avoid possible overlaps of EDS peaks ~~off~~from the coating metals.

After spectra treatment to deconvolve signal from noise (correction for the bremsstrahlung effect, Supplementary Method 1), the colocalisation of SEM images and EDS elemental maps ~~was~~ere done manually using calcium distribution maps (Ca EDS), the main ~~compound component of the test in~~ calcitic ~~tests foraminifera~~ (SEM images). ~~EDS maps~~ Scaling and/or rotation of ~~EDS maps~~ were performed when necessary but deformation (i.e., warping) was never applied. Finally, to obtain a Si ~~mapping from of~~ non-sedimentary origin, ~~the~~ aluminium (Al) signal was subtracted ~~to from~~ the silicon (Si) signal to remove aluminosilicate particles (typically ~~from~~ clay minerals, ~~the~~ major ~~compound constituent of the~~ sediment at the sampling site) from EDS maps. ~~Additional individuals belonging to the genera Uvigerina, Chilostomella and Globobulimina and isolated from the same sample site were also studied with a similar procedure.~~

125 ~~Finally, Additionally,~~ the thickness of the Si layer was measured in each separate chamber (numbered from the proloculus toward the apertural side) on all available *B. spissa* specimens.

Image treatments and measurements were done using the software Fiji (Schindelin et al., 2012).

a mis en forme : Police :Italique

a mis en forme : Police :Italique

a mis en forme : Police :Non Italique

a mis en forme : Police :Italique

2.3 Low-vacuum SEM imaging

130 To expose the Si layer below the calcitic test, isolated and air-dried individuals (n = 15) were subsequently immersed in 0.5 M ethylene-diamine-tetraacetic acid disodium salt solution (EDTA, 03690 - Sigma Aldrich) for 48 h and then rinsed with distilled water before observation. ~~After~~Subsequently, specimens were put on an aluminium stub on carbon tape prior observation with a benchtop SEM (JEOL JCM-6000Plus) in low vacuum mode, without coating, at 15 kV of acceleration voltage and using backscattered electron mode. ~~In addition, optical pictures images~~ using a camera mounted on a stereomicroscope were obtained both before and after ~~the~~ decalcification step. Additional individuals belonging to the genus *Bulimina* and isolated from the same sample site were also imaged with the same procedure.

a mis en forme : Police :Italique

2.4 TEM imaging & EDS measurements

To search for potential organelles involved in biosilicification, we observed the contents of the cytoplasm ~~content~~ using a transmission electron microscope (TEM) and performed high-angle annular dark-field scanning transmission electron microscopy (HAADF-STEM) coupled with EDS analyses. Directly on board, living specimens (n=8) were isolated from different sediment layers of one cm thickness (0-1cm to 4-5 cm depth), ~~isolated and live checked specimens (n=8) and~~ were fixed with glutaraldehyde. Specimens were then embedded in 1 % aqueous agarose and cut into ~ 1 mm cubes. Samples were decalcified with 0.2 % ethylene glycol tetraacetic acid (EGTA) in 0.81 mol L⁻¹ aqueous sucrose solution (pH 7.0) for several days, rinsed with filtered seawater and postfixed with 2 % osmium tetroxide in filtered seawater for 2 h at 4 °C. Samples were 145 rinsed with an 8 % aqueous sucrose solution and stained with 1 % aqueous uranyl acetate for 2 h at room temperature. Stained samples were rinsed with milli-Q water, dehydrated in a graded ethanol series, and embedded in epoxy resin. Blocs were further sectioned into ultra-thin sections (60 nm thick) which were then placed on a formvar-supported copper grid mesh and subsequently stained with 2% aqueous uranyl acetate and lead stain solution (0.3 % lead nitrate and 0.3 % lead acetate Sigma-Aldrich). TEM observations were done with a bottom-mounted 2k × 2k Eagle charge-coupled device (CCD) camera (Tecnaï G2 20, Thermo Fisher Scientific). Elemental compositions were obtained by EDS analyses performed using an EDAX Genesis system under scanning transmission electron microscopy (STEM) mode operating at an acceleration voltage of 120 kV and 200 kV, respectively.

2.5 FTIR spectroscopy

155 The topmost 2 cm sediment from NSB station were sieved on a 63 µm mesh size-sieve and *B. spissa* specimens were isolated from the residue. Only specimens showing a completely empty shell and having a translucent ~~aspect~~ appearance were selected to avoid the presence of remaining cytoplasm in the test. To remove the calcitic layer and expose the underlying Si layer of the test, empty tests were then immersed in 0.5 M EDTA (03690, Sigma Aldrich) for 24 h, rinsed with milli-Q water, placed on a calcium fluoride (CaF₂) plate, and dried in a vacuum chamber prior to measurement. Dried samples were measured using a microscope Fourier transform infrared spectrometer (FTIR 6200 with IRT-7000, Jasco Inc.) with an aperture size of 15 × 15

160 μm . Transmission IR signals were background-corrected to determine the infrared spectra between 4000–750 cm^{-1} spectral region for a total of three specimens. ~~Because~~ CaF_2 absorbs below 1000 cm^{-1} , ~~therefore~~ no band assignments ~~were~~ done in this region (Mayerhöfer et al., 2020).

2.6 Isotopic analyses

In total, 17 specimens of *B. spissa* ~~with transparent shells~~ were isolated from NSB site sediment ([Supplementary Fig. 1](#)). ~~cleaned with Milli-Q water, and carefully examined under a stereomicroscope and to confirm the absence of authigenic particles (Ishimura et al., 2012). Individuals were~~ micro-dissected in two parts using a scalpel aiming to separate the oldest part (proloculus side) from the newest part of the test (apertural side). Because it was challenging to dissect only the proloculus from the other chambers on the apertural side, few chambers were still attached to the proloculus prior ~~measurements to analysis~~ (6 microspheric and 11 macrospherics individuals, [Supplementary Fig. 1](#)). Stable carbon and oxygen isotopic compositions ($\delta^{13}\text{C}$ and $\delta^{18}\text{O}$, respectively) of dissected parts were determined using a high precision microscale carbonate isotopic analytical system, MICAL3c (Ishimura et al., 2004; 2008). Samples were reacted with ~~phosphoric acid (H_3PO_4) to decompose CaCO_3 and produce CO_2 . Note that with the same method, Ishimura et al. (2012) reported that no CO_2 was evolved through the reaction between H_3PO_4 and organic materials at 25°C over several days.~~ After purification, CO_2 was introduced into an IsoPrime100 isotope ratio mass spectrometer (IsoPrime Ltd., Cheadle Hulme, UK) equipped with a customized continuous-flow gas preparation system (MICAL3c) at Kyoto University. This system allows us to determine the $\delta^{13}\text{C}$ and $\delta^{18}\text{O}$ values of as little as 0.1 μg CaCO_3 with an analytical precision of better than $\pm 0.10\%$. The isotopic values were standardised to the Vienna Pee Dee Belemnite (VPDB) scale and expressed in δ notation. The mass of dissected samples was estimated from the volume of CO_2 gas produced during the reaction between CaCO_3 and H_3PO_4 .

3 Results

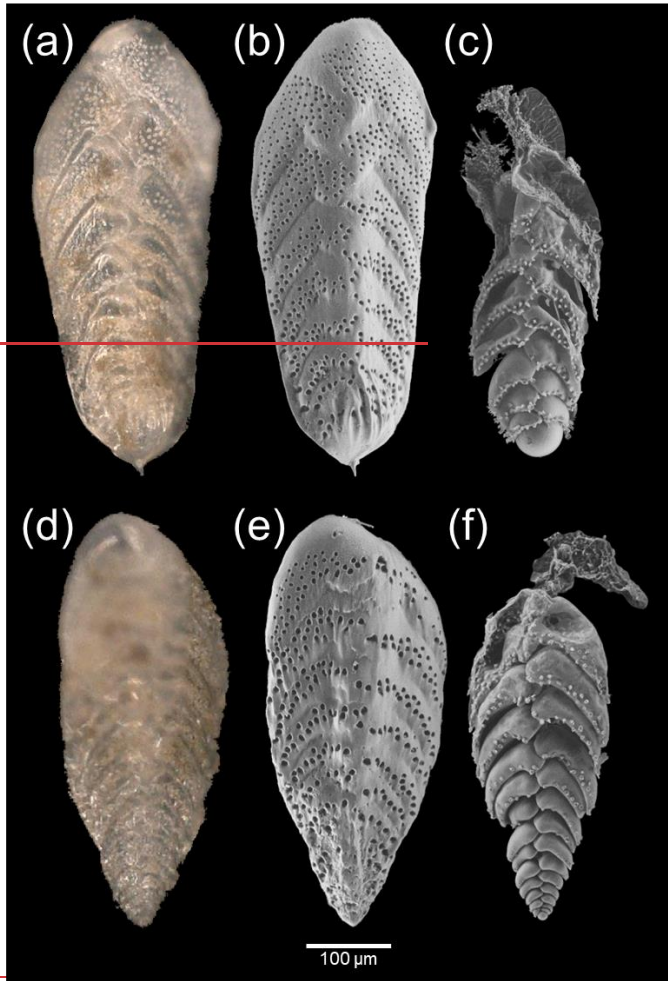
180 3.1 Morphology of the ~~Sisiliteon~~ coating the inside part of the calcitic test

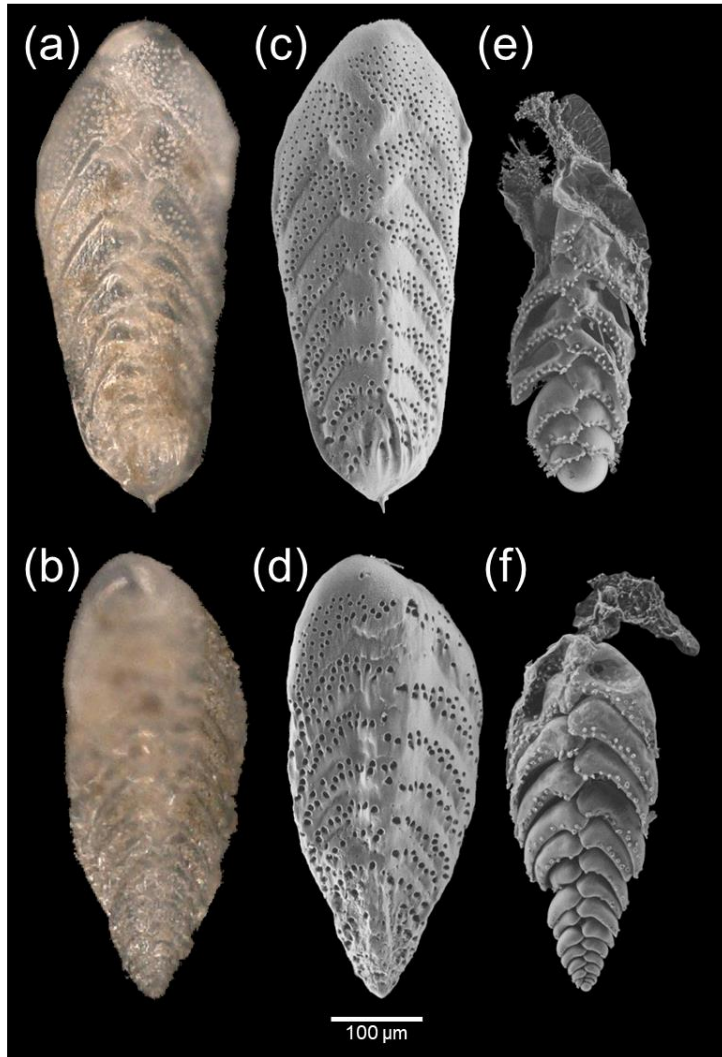
Macrospheric (haploidic) and microspheric (diploidic) specimens were observed with a stereomicroscope (Fig. 2a & 2b) before being imaged in low-vacuum SEM settings (Fig. 2c & 2d). Specimens showed a costate proloculus, acute carinate edges and sometimes a minute apical spike, typical from the morphospecies *Bolivina spissa*. The same specimens were then imaged ~~again in with~~ low-vacuum SEM settings (Fig. 2e & 2f) after the dissolution of their calcitic shell to expose the underlying Si layer. In all individuals, the ~~last few final (newer)~~ chambers were always missing and/or collapsed after decalcification, while the older chambers on the proloculus side remained well shaped (Fig. 2e & 2f).

a mis en forme : Non Exposit/Indice

a mis en forme : Indice

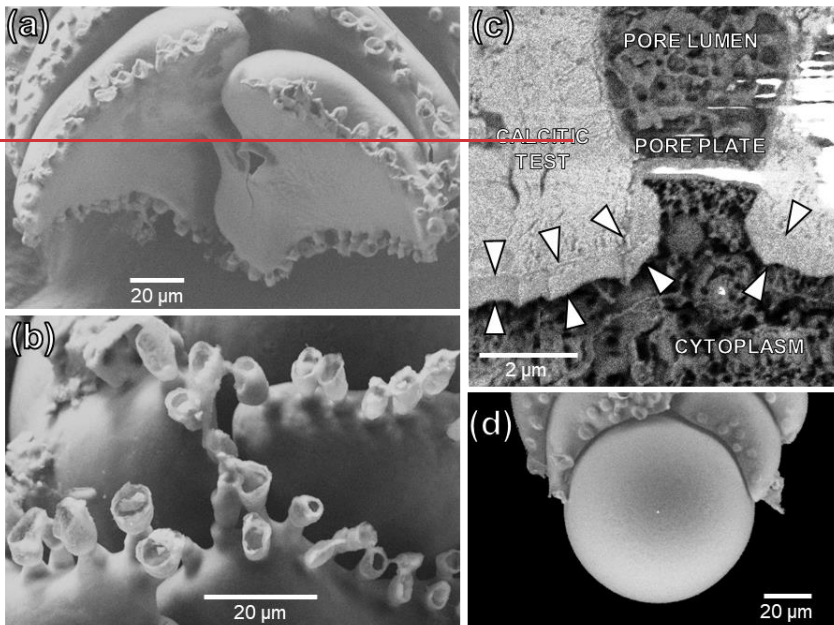
a mis en forme : Indice





190 Figure 2: Macrospheric (top row a–c) and microspheric (bottom row d–f) *Bolivina spissa* specimens, imaged with a stereomicroscope (a and b) and low-vacuum SEM before (c and d) and after (e and f) decalcification to expose the Si layer below the calcitic shell.

Figure 3a shows the Si layer connections between consecutive chambers after the removal of the calcitic test by decalcification. Protruding funnel-like structures were visibly sticking out at the pore-s' location after decalcification, coating the inner surface of the original pore's calcitic wall (Fig. 3b). These funnel-like structures were not made of Si but were probable remains of organic material, as the Si internal coating being visibly terminated at the pore plate from cryo-SEM (Fig. 3c) and TEM observations (Supplementary Fig. 2 & 3) show the Si internal coating terminates at the pore plate. The texture of the Si layer's surface always appeared smooth without visible substructures (excluding where pores priorly occurred), and the proloculus was nearly spherical (Fig. 3d). None of the individuals belonging to the other investigated genera (i.e., *Uvigerina*, *Chilostomella*, *Globobulimina* and *Bulimina*) showed a Si layer.



a mis en forme : Police :Italique

a mis en forme : Police :Italique

a mis en forme : Police :Italique

a mis en forme : Police :Italique

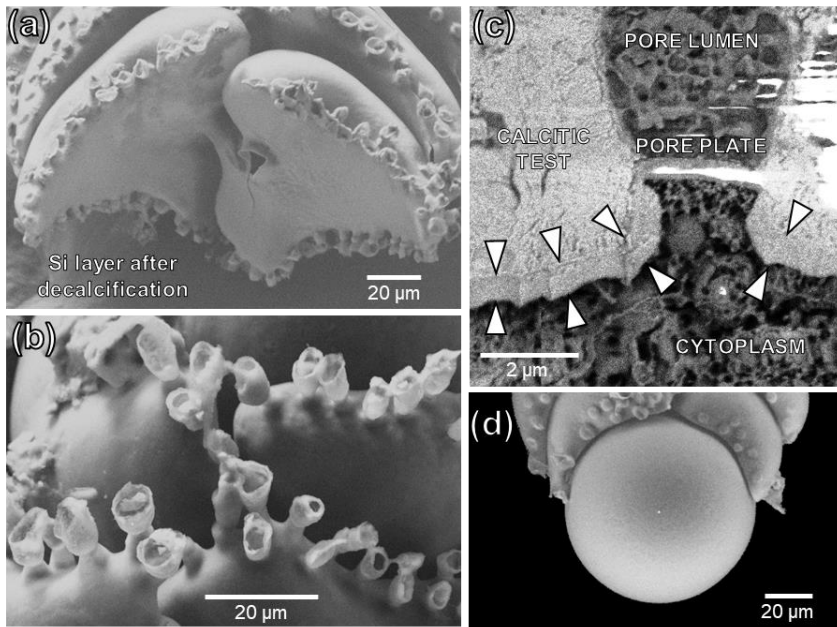


Figure 3: SEM images of the silicified structures of *B. spissa*. (a) Broken *B. spissa* after decalcification to expose the Si layer connections between successive chambers. (b) Magnification on the pore funnel-like structures of *B. spissa* exposed after decalcification. (c) Transversal section of a pore imaged with cryo-SEM on non-decalcified *B. spissa*. White arrows indicate the position of the Si layer. White colour on the top right of the image and on the pore plate is due to overcharging. (d) Magnification of the proloculus of *B. spissa* exposed after decalcification.

Figure 4 illustrates the different steps performed workflow used to obtain the Si distribution maps from non-sedimentary origin which were finally superimposed on the cryo-SEM images. The calcium distribution (Fig. 4a & 4b) followed the electron-dense area SEM images (Fig. 4c & 4d) representing the calcitic test of individuals (Fig. 4a-d). Sedimentary aluminosilicates were removed by subtracting the aluminium signal from that of siliceous-Si (Fig. 4e-j), and the resulting signal showed that the siliceous-Si was localised on the inner wall of the calcite test (Fig. 4k-l). The Si lining from non-sedimentary origin was systematically found in all the seven specimens analysed (Table 1) and the Si signal was always stronger in the older chambers (proloculus side) than in the newer chambers (aperture side, Fig. 4i-2l).

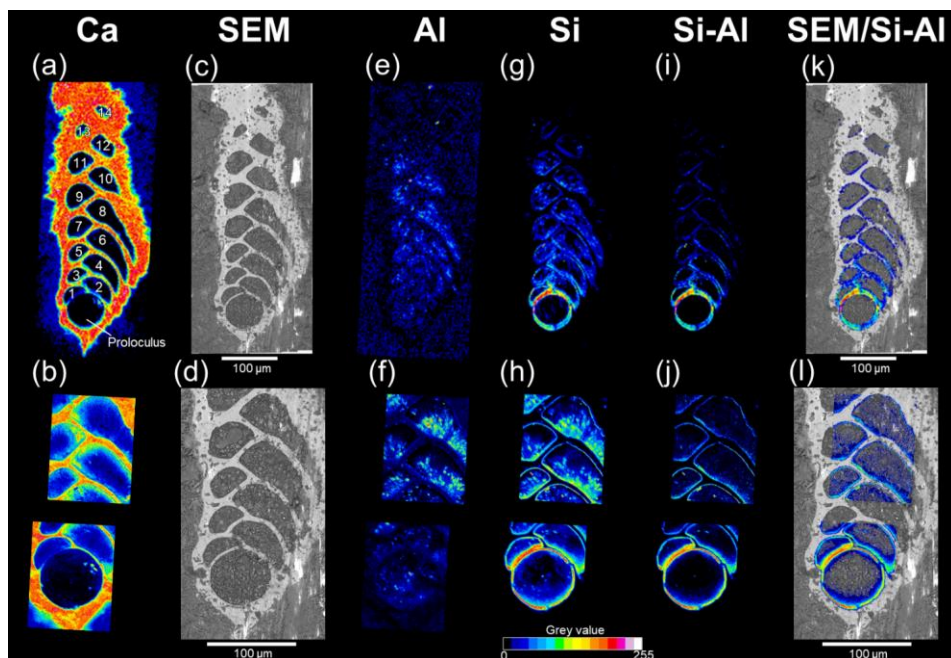


Figure 4: SEM imaging and EDS maps (16 colours grey value scale) of a representative cryo-fixed *B. spissa* (a, c, e, g, i and k) and magnification on areas of interest (b, d, f, h, j and l). (a and b) EDS maps of Ca used to colocalise EDS elemental maps and SEM images. **P**The proloculus is indicated and chambers are numbered. (c and d) SEM images of a cryo-cracked specimen. (e and f) EDS maps of Al (g and h) EDS maps of Si. (i and j) Resulting EDS maps from the subtraction of the Al signal **to-from** the Si signal (i.e., removing aluminosilicates). (k and l) Superimposition of Si map **from-of** non-sedimentary origin over SEM images.

The Si layer was clearly identifiable on cryo-SEM images as a less electron-dense structure coating the internal part of the calcitic test (Fig. 5). The thickness of this Si layer was constant inside individual chambers for a given specimen. The decreasing Si signal from **the** proloculus **toward** apertural side detected on EDS maps (Fig. 4i-l) was confirmed by **cryo-SEM** observations **on cryo-SEM images as visible showing** decreasing Si layer thickness **of the layer toward younger chambers** (Fig. 5). The Si layer was homogeneous without any visible layering even on the thickest sections and exhibited conchoidal fractures which is typical for glassy **nature** materials (Fig. 5e). No other visible structures **were as** observed between the Si layer structure **and** the calcitic shell, which were in direct contact. In very rare cases, we observed a **hollow part gap** between the two layers such as **in** Fig. 5e, that we ascribe to preparation artifacts (i.e., **the** cutting step).

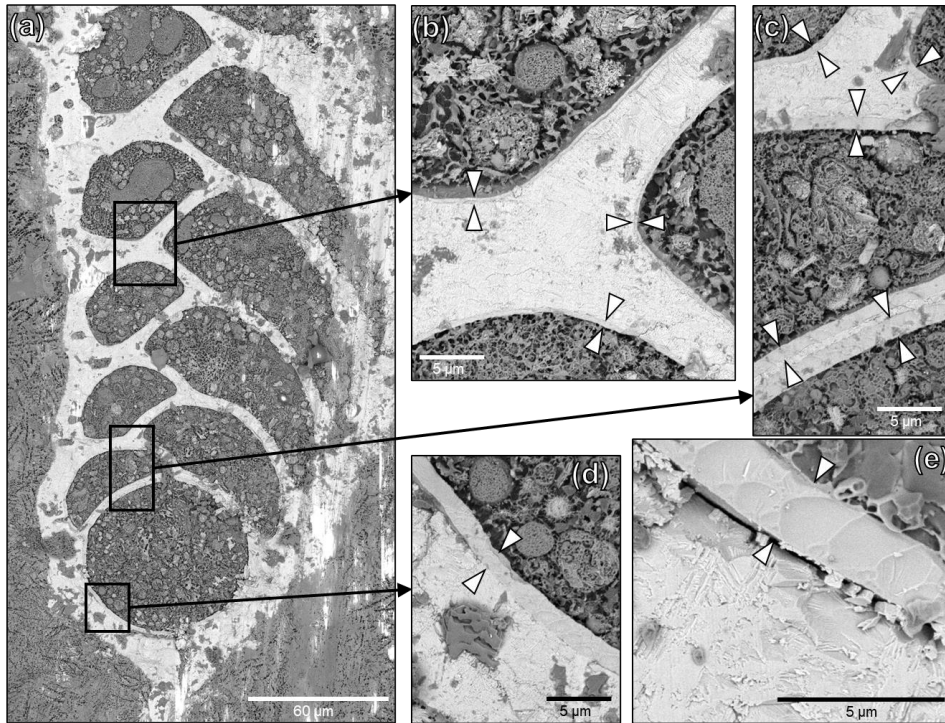


Figure 5: Cryo-SEM images of a representative cryo-cracked *B. spissa* specimen. (a) Overview of the specimen and (b–e) magnified regions of interest (black squares) to visualise the Si layer (indicated by white arrowheads) coating the inside part of the calcitic test. Note the decreasing thickness of the layer from the proloculus toward newer chambers. (e) Magnified cryo-SEM image of the Si layer in the proloculus showing the homogeneity of the structure. Note the conchoidal fracture pattern typical from of glassy nature materials. The hollow part gap between the calcitic shell and the Si layer was very rarely observed and is resulting from the cutting steps preparation artifact.

The thickness of the Si layer was equivalent considering each separate chamber and ranged from 1.65 to 0.05 μm , respectively measured in the proloculus part and in the last chamber of the individual where the Si layer was still visible (Supplementary Table 1). Data presented here must be considered carefully because a sub-perpendicular cracking orientation could introduce a bias in the actual thickness of the Si layer in each specimen. The Si layer was not visible in chambers newer younger than chamber 12 while when the number of visible chambers was higher than 12 in five over of the seven specimens (Supplementary Table 1). However, the cryo-SEM image resolution definition might have not been sufficient to detect structures smaller than 0.05 μm , corresponding to about four pixels in the acquired images. Thickness data indicated that the decreasing trend in the Si layer thickness follows an inverse power law ($r^2=0.99$, Fig. 6).

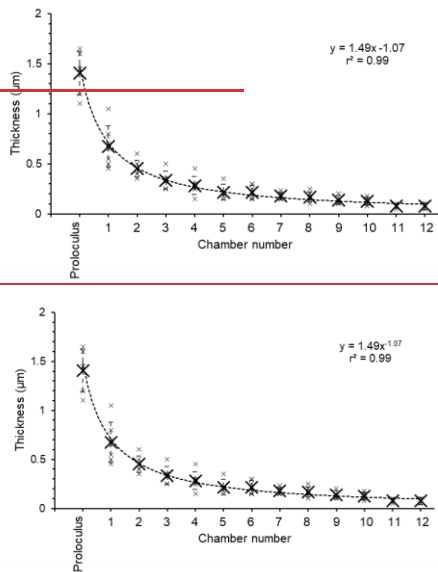
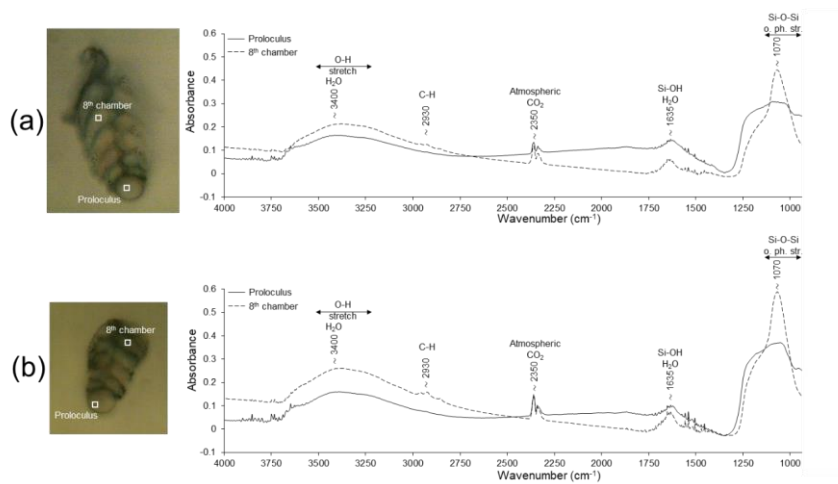


Figure 6: Plot representing the thickness of the Si layer as a function of the chamber number (numbered such as indicated on Fig. 4a) measured on 7 individuals. Measurements (small black crosses) were averaged by chamber (big black crosses) and the standard deviation is represented by error bars. The black dotted line is a power law trend line based on averaged values.

3.2 Infrared spectra analyses

For all three *B. spissa* specimens and all chambers, FTIR spectra (Fig. 7) displayed a strong absorption band at $\sim 1070\text{ cm}^{-1}$ with an associated shoulder at $\sim 1250\text{ cm}^{-1}$ that are attributed to the asymmetric Si-O-Si stretching vibrations (Socrates, 2004; Larkin, 2011). The broad band at 3400 cm^{-1} and at $\sim 1635\text{ cm}^{-1}$ are ascribed to the O-H stretching of absorbed water (Socrates, 2004; Larkin, 2011), matching with opal. The IR spectra from the proloculus showed a broader band at $\sim 1070\text{ cm}^{-1}$ with a shoulder at $\sim 1250\text{ cm}^{-1}$, while a small peak from C-H stretching was observed at $\sim 2930\text{ cm}^{-1}$ in spectra of the 8th chamber.



255 | **Figure 7: Examples of Representative FTIR spectra measured on the proloculus (solid line) and the 8th chamber (dotted line) for two decalcified specimens (a and b) of *B. spissa*. o. ph. str. = out of phase stretching.**

3.3 TEM imaging & STEM-EDS measurements

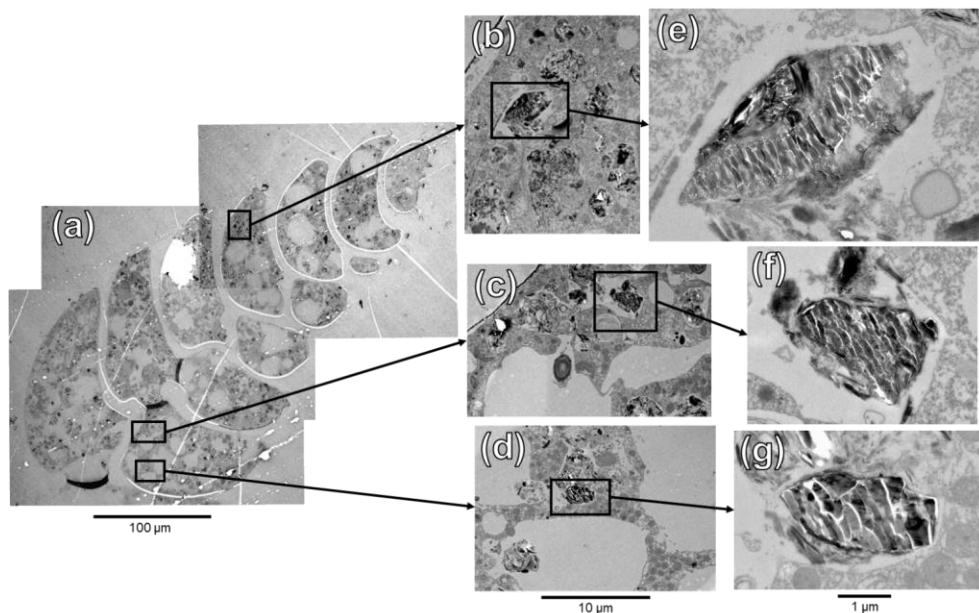


Figure 8: TEM images of ultra-thin section of *B. spissa* specimen (a). (b–d) Magnified regions of interest represented by black squares on (a). (e–g) Further magnified area of the black squares in (b), (c) and (d) respectively.

260 To investigate the putative organelles involved in silica deposition, TEM imaging of ultra-thin sections of *B. spissa* individuals were performed imaged with TEM (Fig. 8a). On-From a total of eight individuals imaged, two showed structures filled with material presenting showing the characteristic conchoidal fracture pattern of siliceous-Si-based materials (Fig. 8b–g) were observed in two individuals. This conchoidal fracture pattern when sectioned with a diamond knife was also clear on the Si layer coating the inside part of the calcitic shell, which was visible on all eight specimens (Supplementary Fig. 2). Note that the aspect-appearance of these structures on TEM images is presumably denatured during sample preparation, such as previously reported for other silicifying organisms (Garrone et al., 1981).

265 STEM-EDS analyses indicated that the electron-dense material in these vesicles was mainly composed of siliceous-Si and showed a similar spectrum to the Si layer coating the internal part of the calcitic test (Supplementary Fig. 4). These organelles are remarkably resembling-similar to Silica Deposition Vesicles (SDVs) described in other biosilicifying organisms (Anderson, 1994; Foissner et al., 2009). The elemental composition of the content of these SDV-like organelles was different from vesicles filled with sediment material where Si was mostly associated with Al (aluminosilicates, such as feldspars which are abundantly

found in the sediment, Supplementary Fig. 4). The latter vesicles, filled with sediment and organic detritus, ~~occur~~ abundantly ~~occurring~~ in the cytoplasm of *B. spissa* and represent food vacuoles (Goldstein & Corliss, 1994).

3.4 Isotopic analyses

275 The calcite mass of dissected samples ranged between 0.2 µg to 2.9 µg for ~~the~~ proloculus side and 1.1 µg to 13.6 µg for ~~the~~ apertural side (Supplementary Table 2). The proloculus side of dissected samples exhibited low $\delta^{18}\text{O}$ values ~~between-ranging~~ ~~from~~ +0.13‰ to +3.09‰ compared with the aperture side which ~~was ranging~~ ranged from +2.11‰ to +3.11‰. The $\delta^{18}\text{O}$ values of aperture side ~~were~~ comparable ~~with-to the~~ isotopic equilibrium value of calcite at ~~the a~~ depth of 1100 m in ~~the~~ Sagami Bay (Ishimura et al., 2012). Specimens exhibiting low $\delta^{18}\text{O}$ values also ~~showed~~ represent low $\delta^{13}\text{C}$ values. This trend was
280 observed both for microspheric and macrospheric individuals (Supplementary Fig. 5). Lower $\delta^{18}\text{O}$ and $\delta^{13}\text{C}$ values were typically found in smaller (i.e., younger) specimens, having a test length ranging from 200 to 400 µm (Supplementary Fig. 6).

4 Discussion

4.1 Composite test made of calcite and opal

The Si layer, which was systematically observed in all studied *B. spissa*, is composed of biogenic opal (amorphous hydrated
285 silica, $\text{SiO}_2 \cdot n\text{H}_2\text{O}$). This was firstly indicated by the cross-sections of the ~~silicon~~ ~~Si-rich~~ layer exposed by diamond knife cutting ~~on~~ (cryo-SEM and TEM images), both showing a conchoidal fracture pattern (Fig. 5e & Supplementary Fig. 2), typical ~~from~~ ~~of~~ amorphous glass and well known ~~from-for~~ a variety of ~~silicon~~ ~~Si-based~~ ~~using~~ organisms (see review in Garrone et al., 1981). This was further confirmed by FTIR spectra obtained on decalcified empty tests (translucid, dead), which were ~~perfectly~~ ~~matching~~ ~~in good agreement with spectra of~~ reference opal (Lowenstam, 1971), diatom frustules (Stefano et al., 2005) and
290 diatomite (Reka et al., 2021) spectra. This is congruent with previous measurements on *Miliammellus legis* in Resig et al. (1980), for which the test material spectra also matched the opal reference of Lowenstam (1971).

The opal layer coating the inside part of the calcitic test of *B. spissa* ~~seems composed of~~ ~~appears~~ homogeneous ~~material~~, without any visible sub-structures even on high resolution SEM images. This is different from *M. legis*, for which the test, made entirely of opal, is formed by a median layer (18 µm thick) composed of fused tubular rods randomly arranged in three-dimensional
295 open mesh. ~~This median layer is~~, framed by an inner and an outer layer (1 µm thick each), both composed of tightly packed rods sheets parallel to the inner and outer surface of the shell, respectively (see Plates 2 & 3 in Resig et al., 1980). These morphological and structural differences suggest different precipitation processes between the two genera, ~~such as it~~ is the case for the carbonate ~~tests of~~ ~~the~~ Miliolida and Rotaliida, to which *Miliammellus* and *Bolivina* respectively belong (Parker, 2017; Dubicka, 2019).

300 In *B. spissa*, the opal layer thickness was constant within each chamber but was not equivalent between chambers in a given individual, always being the thickest in the proloculus and becoming thinner toward the newer chambers at the apertural side of the test. This decreasing trend in thickness is ~~analogous~~ to the calcitic tests in Foraminifera having a lamellar wall (such

as *Bolivina*), which cover the entire test with new calcitic material (i.e., outer lamellae) when adding a new chamber, resulting in a decreasing thickness of the calcitic test from the proloculus toward the newest chamber (Hansen, 2003). ~~The outer lamellae covering the entire test when adding a chamber is progressively decreasing in thickness, so that the more layers are added, the more increasingly difficult it becomes to trace (Bé & Lott, 1964).~~ In some of our *B. spissa* specimens, we ~~could~~ observed such a decreased outer lamellae thickness toward external calcite layers on cryo-SEM images. The opal layer thickness from the proloculus towards the apertural side of the test follows an inverse power law (Fig. 6), suggesting that it ~~is resulting results~~ from an ontogenetic effect. This decreasing thickness trend, ~~similarity~~ in both calcite and opal, coupled to the observation of ~~an~~ opal coating in young specimens (i.e., with few chambers), indicates that the opal layer is not formed during a single event but during multiple discrete steps, ~~possibly likewise comparable to~~ the precipitation pattern for the calcitic test. However, even in the proloculus where its thickness is ~~at a~~ maximum, no layered sub-structures were visible in the opal layer (Fig. 3d & 5e). After decalcification, the ~~few last youngest~~ chambers on the apertural side were always collapsed or absent (Fig. 2e & 2f), either because the opal layer was too thin to maintain its chamber-shaped structure or because of its absence in the newest part of the test. This is corroborated by cryo-SEM and TEM images observations, where no opal layer was visible in the newest chamber(s) (Fig. 5a & 8a; Supplementary Fig. 7). The absence of ~~an~~ opal layer in the newest calcified chambers indicates that its formation must occur after ~~ward~~ the precipitation of the calcitic shell.

4.2 Is ~~it~~ the opal layer precipitated by the foraminifera itself?

Several observations indicate that the opal layer is secreted by the foraminifera itself and is not due to specific environmental conditions or any other passive process(es):

1. The layer is systematically present in all *B. spissa* sampled during two consecutive years (May and October 2022 and May 2023) and isolated from different depth intervals in the sediment, ~~and~~ hence exposed to different environmental conditions (e.g., oxic/anoxic).
2. The layer only coats the inside part of the calcitic shell, suggesting that it is resulting from a mechanism taking place inside the calcitic test (i.e., in the cell and not in the surrounding water).
3. The layer is observed in living specimens, ~~showing demonstrating~~ that the deposition process occurs ~~while~~ the individual is alive.
4. The layer is not observed in any other species found at the same site, such as ~~individuals belonging to~~ *Uvigerina*, *Chilostomella*, *Globobulimina* or *Bulimina* genera, indicating that opal formation in *B. spissa* is not the result of a passive process.
5. The smooth and homogeneous ~~aspect appearance~~ of the layer suggests that it is resulting from a precipitation process and not ~~from of~~ an aggregation of particles from allochthonous origin (e.g., ~~of sedimentary~~ or biogenic ~~origin, but~~ ~~i.e.,~~ ~~previously~~ secreted by another organism and subsequently incorporated by the foraminifer).

a mis en forme : Police :Non Gras, Non Italique, Couleur de police : Automatique

a mis en forme : Police :Non Gras, Non Italique, Couleur de police : Automatique

a mis en forme : Police :Non Italique, Couleur de police : Automatique

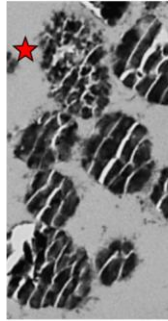
335 6. The opal layer thickness follows an allometric relationship (i.e., inverse power law), from the proloculus (thick) to newer chambers (thin), commonly found in organisms' growth patterns and suggesting that the layer is resulting from an ontogenetic process, analogous to the secreted calcitic test.

Supplementary TEM observations reveal ~~of~~ peculiar organelles occurring in the cytoplasm, ~~containing material exhibiting the typical conchoidal fracture pattern on TEM images and opal composition in EDS spectra (Fig. 8 & Supplementary Fig. 4). These findings and filled with similar material to opal layer (i.e., typical conchoidal fracture pattern on TEM images and EDS spectra indicating opal composition, Fig. 8 & Supplementary Fig. 4)~~ further corroborate ~~the assertion~~ that the foraminifer secrete the opal layer itself ~~(Fig. 8 & Supplementary Fig. 4)~~. These organelles are strikingly ~~resembling similar to~~ Silica Deposition Vesicles (SDVs), involved in the secretion of opal in ~~diatom's frustules of diatoms~~ (Drum & Pankratz, 1964) or the shell ~~building~~ of other organisms in the SAR group (Anderson, 1994; Foissner et al., 2009; Fig. 9) to which Foraminifera belong. While *B. spissa* was shown to feed selectively on fresh phytodetritus transported from the surface ocean (e.g., diatoms, Nomaki et al., 2006), the ~~aspect-appearance~~ of these organelles greatly differs from typical diatom frustules ingested by foraminifera (e.g., see Fig. 9D in Jauffrais et al., 2018, Fig. 4D in Goldstein & Corliss, 1994; Supplementary Fig. ~~87~~ in this study) or sponge spicule (Garrone et al., 1981) indicating that they do not represent remains from these organisms. We consider that these organelles are SDVs (Fig. 8 and 9), which ~~were-have~~ never ~~been~~ reported before in Foraminifera (see review in LeKieffre et al., 2018). The observation of these SDVs-like organelles in two ~~out~~ ~~of~~ ~~ver~~ eight individuals analysed in total supports the hypothesis that the opal deposition process takes place intermittently, or that these organelles occur rather rarely in the cytoplasm of *B. spissa*. SDVs-like organelles were observed ~~both~~ in ~~younger~~ ~~new~~ and older chambers ~~at the same time of the same specimen~~ (Fig. 8), suggesting that ~~the~~ opal layer deposition might occur simultaneously in different chambers, resulting in thicker layers in older chambers. These organelles were observed in individuals from 1-2 cm depth interval in the sediment, where oxygen is absent (Glud et al., 2009), suggesting that opal precipitation may occur in anoxic settings, ~~as it was shown for calcite precipitation (Nardelli et al., 2014; Orsi et al., 2020)~~. Further analyses, such as a transcriptomic study targeting genes involved directly in silica precipitation or biosilicification, are necessary to conclude about the exact nature of these organelles.

The existence of a secreted opal layer coating the inside part of the calcitic test highlights a new biosilicification process in *B. spissa*, making this species the first Rotaliida able to secrete opal and the first Foraminifera able to precipitate both materials (i.e., calcite and opal) ever reported ~~on~~ in ~~our knowledge~~ ~~the literature~~.

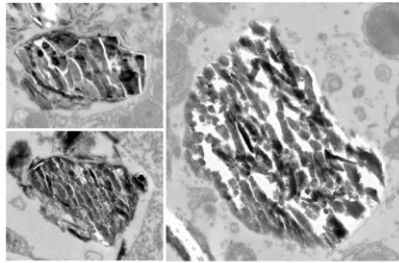
Ciliate SDVs
Maryna umbrellata
(Foissner et al., 2009)

Final developmental stage
Silicon granules showing typical conchoidal fracture pattern of glass. One of the granule was pulverized by the diamond knife (red star)



1 μ m

Putative Foraminifera SDVs
Bolivina spissa
(this study)



2 μ m

Figure 9: TEM images showing the final development stage of the silicon-Si granules in SDVs in the ciliate *Maryna umbrellata* (modified from Foissner et al., 2009) and organelles in *B. spissa* exhibiting similar aspect/appearance, hence representing putative SDVs. Note the scale difference, which is two times larger for *B. spissa* than for the ciliate.

365 The only other known biosilicifying Foraminifera is *M. legis* (Miliolida, Burmistrova, 1978), which is branching relatively far from *Bolivina* (Rotaliida) in phylogenetic trees based on 18S rRNA (e.g., Pawlowski et al., 2013) or multi-gene phylogenies (Groussin et al., 2011; Krabberød et al., 2017; Sierra et al., 2022, Supplementary Fig. 98a). These phylogenetic relationships, nesting-in which Rotaliida and Miliolida are nested within naked foraminifers, suggests that biosilicification was acquired independently throughout their evolution history. Similarly, it was-has been already-previously suggested that different test organisation/composition and calcification pathways likely emerged multiple times during foraminiferal evolution in different foraminiferal orders, especially between Rotaliida and Miliolida (Groussin et al., 2011; Pawlowski et al. 2013; Holzmann & Pawlowski, 2017; Sierra et al., 2022, de Nooijer et al., 2023). The distinct appearance/aspect and microstructure of the opaline shell found in *B. spissa* compared to *M. legis* supports the idea that this trait emerged independently in both *Bolivina* and *Miliammellus*. However, we cannot exclude the hypothesis that biosilicification was inherited from a common ancestor (of rhizarians for instance) and that this trait was lost in most of other Foraminifera represents. Silicon Transporter (SIT) genes putatively inherited from a common eukaryotic ancestor were-alreadyhave previously been identified in other well studied rotaliid Foraminifera that are not known to exhibit any opaline silica structures (i.e., *Ammonia*, *Elphidium* and *Rosalina*, Marron et al., 2016, Supplementary Fig. 98b). This finding confirms that the presence of *SIT* genes does not necessarily imply the capacity to precipitate opaline silica and rather corroborates the common ancestor hypothesis. To investigate the exact origin of biosilicification in Foraminifera from an evolutionary point of view, further extensive phylogenetic studies including *M. legis* are urged.

4.3 Function(s) of the opal layer

The calcitic shell of Foraminifera test may potentially originate from the detoxification of harmful Ca^{2+} ions within the cell (Simkiss, 1977; Kaźmierczak et al., 1985), the resultant test was proposed to serve various functions such as protection against predation, buoyancy control, or facilitation of reproduction. Similarly, the opal layer may also be initially secreted as a detoxification byproduct (Marron et al., 2016), with additional function(s) beneficial for their success in deep-sea environments. Undoubtedly, the test also acts as protective physical barrier against unfavourable physical or chemical conditions of the environment (Marszalek et al., 1969; Wetmore, 1987), particularly considering the chemical and mechanical characteristics of opal.

The only other foraminifer having an opaline test, *M. legis*, is found in relatively deep habitats (> 4400 m depth, Burmistrova, 1978; Resig et al., 1980) below the Carbonate Compensation Depth (CCD) where calcitic foraminifera are very rare (Resig et al., 1980; Gooday et al., 2008). This suggests that secreting an opaline test could be an adaptation in environments in which producing and maintaining a calcitic shell is challenging. However, *B. spissa* specimens in the present study were found at much shallower depths (1410 m) well above the CCD (~ 4500-5000 m depth in the northwest Pacific, Chen et al., 1988), in samples where other calcitic species occur abundantly and without any visible signs of dissolution. This indicates that calcification is not limiting in these environments and suggests that the opaline and calcitic parts of the test could serve different and/or complementary function(s).

Diatom frustules, made of opal, are known to possess incredible mechanical properties are reportedly known to achieve incredible mechanical properties regarding their light weight and such as remarkable light weight, strength leading to remarkable structural integrity and structural integrity, (among other functions; Hamm et al., 2003; Knoll & Kotrc, 2015; Aitken et al., 2016). Despite Even if we did not observe any microstructures in the opal layer of *B. spissa* such as in diatom's frustules it is plausible that the opal layer may serve as a supplementary mechanical support for the calcitic shell, enhancing the mechanical integrity of the entire test. While However, this hypothesis is not supported by the occurrence of other species having a more fragile test compared to *B. spissa* at the same location, such as *Chilostomella*, does not support this hypothesis, it still needs to be invalidated with measurements. Achieving a better mechanical resistance regarding compressive forces could represent an advantage in the context of protection against potential predation. This might be especially true for propagules or juveniles, since the opal layer is the thickest in old chambers at the proloculus side.

The thick opal layer in the proloculus might indicate a function associated with propagules dispersion. Compared to calcite, opal has a lower density (2.7 $\text{g}\cdot\text{cm}^{-3}$ and 1.9-2.2 $\text{g}\cdot\text{cm}^{-3}$, respectively, Mukherjee, 2012), which could facilitate resuspension, movements, and/or propagation of juveniles by decreasing the density of young tests compared to a test of equivalent thickness made only of calcite. Some benthic foraminiferal species are hypothesised to have a floating propagule stage to insure long-distance dispersal to different habitats (Alve & Goldstein, 2010). Alternatively, another *Bolivina* species, *Bolivina variabilis*, was reported as having a tychoipelagic life strategy and being able to grow and calcify in benthic and in planktic settings depending on its ontogenetic stage (Darling et al., 2009; Kucera et al., 2017). The low $\delta^{18}\text{O}$ in the proloculus part of *B. spissa*

a mis en forme : Exposit

415 (Supplementary Fig. 6 and 7) could indicate that juvenile specimens did calcify ~~in a~~ higher temperatures ~~environment~~ compared to adult chambers, such as ~~it~~ is the case for the congeneric *B. variabilis* (Darling et al., 2009). However, the isotopic shift between old and new chambers was not observed systematically in *B. spissa*, even among small individuals. Finally, the fact that an opal layer was not observed in decalcified *B. variabilis* (Supplementary Fig. 109) does not support the hypothesis that the opal layer observed in *B. spissa* could be involved in buoyancy function.

420 Opaline silica is acid-resistant and ~ 5 times ~~harder~~ ~~more resistant~~ to abrasion than calcite (Mukherjee, 2012). These two parameters might be of great value regarding protection against ~~foraminifer~~ ~~very~~ ~~predation~~ (Hickman & Lipps, 1983). For instance, parasitic Foraminifera were reported to ~~be able to~~ drill holes into the shells of bivalves by corrosion (i.e., dissolution, Cedhagen, 1994) and into the calcitic tests of other Foraminifera species (by unknown mechanism, Hallock & Talge, 1994). Drilling by mechanical abrasion, presumably the result of predation by nematodes, was also found on foraminiferal tests belonging to *Rosalina* and *Bolivina* genera (Sliter, 1971). Additionally, selective predation on ~~a~~ Foraminifera from the Galapagos hydrothermal mounds by a naticid gastropod was reported by Arnold et al. (1985) and other unknown organisms were suggested to bore holes into foraminiferal tests (Nielsen, 1999; Hickman & Lipps, 1983). Drilling strategies, either by chemical etching or mechanical abrasion, would be much more difficult or even inefficient against an opal layer, which would act as a protective ~~veon~~ layer preventing predators ~~from~~ ~~to~~ ~~accessing~~ the cell content. Foraminifera in the Sagami Bay ~~were shown~~ ~~to~~ ~~bear~~ potential prey for a variety of metazoans (e.g., molluscs, copepods, or nematodes, Nomaki et al., 2008), supporting the protection against predation hypothesis for *Bolivina* in this study. In case of complete ingestion by another organism (deliberate or fortuitous, e.g., Herbert, 1991; Hickman & Lipps, 1993; Lipps, 1983), ~~it was suggested that~~ some Foraminifera may survive relatively short passage in the gut by retracting in their test (Culver & Lipps, 2003), and the opaline silica layer may further help to avoid complete dissolution of the test in that specific case. Environmental SEM observations performed on another *Bolivina* morphospecies sampled from a nearby site in ~~the~~ Sagami Bay (Off Misaki, 740 m depth, 35°04.30' N 139°32.50' E) indicate that it possesses comparable structures to *B. spissa* underlying the calcitic test after decalcification (Supplementary Fig. 110). While these observations were only made on few dead specimens, we ~~sometimes~~ ~~occasionally~~ observed ~~such~~ predatory marks on their tests, with the calcitic test being totally bored but with an underlying layer incompletely pierced (Supplementary Fig. 121). ~~While~~ ~~Although~~ these observations were made on a different *Bolivina* morphospecies, it suggests that protection from drilling strategy occur at a nearby location for the same genus. However, additional studies are necessary to confirm the exact nature of the structure exposed after decalcification in this different morphospecies and the origin of these borings.

440 We hypothesise that a plausible function of this opal layer coating the inside part of the calcitic shell would be ~~an anti~~ ~~predatory~~ ~~function~~ ~~for~~ ~~protection~~ ~~against~~ ~~predators~~, efficient against chemical or abrasive boring attacks, and potentially increasing the overall strength of the test in case of important compressive mechanical stress. Further investigations are needed to validate this hypothesis and define ~~potential~~ ~~possible~~ other(s), ~~and~~ ~~perhaps~~ ~~potentially~~ non-exclusive, function(s).

4.4 Implication(s) for palaeoproxies and biogeochemical cycles

Compared to the aperture side of *B. spissa* where C and O isotopic compositions were ~~almost~~ close to equilibrium values, lower calcitic $\delta^{13}\text{C}$ and $\delta^{18}\text{O}$ values were principally observed at the proloculus side where the Si layer is the thickest. Moreover, the isotopic values of the proloculus side may be overwritten/diluted by the deposition of secondary calcite added during growth, lowering even further the $\delta^{18}\text{O}$ and $\delta^{13}\text{C}$ isotopic ratios that were measured in this study. This is confirmed by the fact that small specimens (i.e., with fewer chambers, younger) showed lower $\delta^{13}\text{C}$ and $\delta^{18}\text{O}$ values compared to larger specimens (i.e., with more chambers, older). These offsets can be explained by either “vital effects” during calcification or different habitat temperatures during the juvenile stage. Alternatively, the higher silicification observed on the proloculus side compared to the aperture side may possibly have altered the cytoplasmic activity and/or resource partitioning regarding C and O in the cell, explaining the differences in isotopic composition between old and new chambers. Ishimura et al. (2012) suggested that the variations of intracellular chemistry affect the isotopic composition of the calcite shell. This may/might result from the more intense Si precipitation on the proloculus side (thicker opal layer) compared to the apertural side of the test in *B. spissa*, assuming simultaneous calcite precipitation and opal formation within putative SDVs. However, the decreased $\delta^{18}\text{O}$ values in the proloculus part of *B. spissa* was not observed in all specimens, suggesting there could be other mechanism(s) responsible for such light isotopic compositions. Increasing the number of specimens analysed and conducting high spatial resolution analyses of isotopic compositions, such as Secondary Ionisation Mass Spectrometry (SIMS) or laser ablation ICP-MS, will provide further insight into a potential isotopic composition shift regarding chamber position. Additionally, the presence of an opaline layer might possibly influence proxy calibrations and their interpretations by mixing the measured calcite signal with the opal signal, such as suggested for sedimentary silicate grains incorporated within the calcite of *M. barleeanus* (Borrelli et al., 2018). The test composition of calcitic foraminifera is widely used for palaeoreconstruction and palaeoproxy purposes (e.g., Zachos et al., 2001; Katz et al., 2010) and *B. spissa* was already has been used in this context (Glock et al., 2012; Koho et al., 2017). Therefore, refined geochemical composition analyses of the opaline layer, not done-performed in our study, are necessary to assess its impact in the context of the use of *Bolivina* shells as a geochemical palaeoproxy. On the other hand, the presence of this opaline layer may open a whole new opportunity to develop novel proxies based on the glassy part of *B. spissa* test, especially in oxygen depleted environments. Such proxies exist for instance for diatoms, silicifying sponges or radiolarians, for which the isotopic composition may be used to trace dissolved silica concentration, pH or nitrate utilisation through geological times (e.g., De La Rocha, 2006; Hendry et al., 2010; Donald et al., 2020; Trower et al., 2021).

Bolivina spissa is a cosmopolitan shallow infaunal species regularly reported at several different locations in the north-east Pacific such as the Santa Monica Basin, Monterey Bay cold-seeps or at the Cascadia convergent margin (e.g., Cushman, 1926; Bernhard et al., 2001; Heinz et al., 2005; Keating-Bitongo & Payne, 2017) as well as in the south-east Pacific at the Peruvian margin (Glock et al., 2011). The species is also found in the north-west Pacific around Japan (Kitazato et al., 2000; Nomaki et al., 2006; Glud et al., 2009; Fontanier et al., 2014; Koho et al., 2017) and in the Okhotsk Sea (Bubenshchikova et al., 2008).

a mis en forme : Police :Italique

480 ~~Foraminifera are known to be major protagonists contributing to the organic and inorganic carbon cycle (OM degradation e.g., Gooday et al., 1992; Moodley et al., 2000; carbonate production, e.g., Langer, 2008) and nitrogen cycle (for denitrifying species such as *B. spissa*, e.g., Pina-Ochoa et al., 2010; Xu et al., 2017; Glock et al., 2019; Woehle et al., 2022). The wide geographic distribution and abundance of *B. spissa* emphasise its potential to be a good palaeoproxy using its opaline test ~~and for global nitrogen cycle.~~ Foraminifera are known to be major protagonists contributing to the organic and inorganic carbon~~
485 ~~cycle (OM degradation e.g., Gooday et al., 1992; Moodley et al., 2000; carbonate production, e.g., Langer, 2008) and nitrogen cycle (for denitrifying species such as *B. spissa*, e.g., Pina-Ochoa et al., 2010; Xu et al., 2017; Glock et al., 2019; Woehle et al., 2022). Furthermore, prior TEM observations of *Bolivina pacifica* (Fig. 4 in Bernhard et al., 2010) and *Bolivina argentea* (Figure 1a in Bernhard et al., 2012) revealed similar structures to those observed in *B. spissa* in this study, suggesting the potential presence of an opal layer beneath the calcitic test of other *Bolivina* species. If silicification in foraminifers was finally~~
490 ~~found to be more widespread than previously known, either among the genus *Bolivina* or possibly among other Foraminifera genera, this group could also have a substantial but overlooked participate role in silicon-Si cycling, adding up to the already significant role of other Rhizaria in this cycle (Llopis Monferrer et al., 2020). Overall, silicifying Foraminifera may represent a critical component to better understand global Si cycling, which is in turn crucial to comprehend the functioning of other biogeochemical cycles, biological carbon pump or marine food webs (Tréguer et al., 2021).~~

495 5 Conclusions

We report that the Foraminifera *Bolivina spissa* exhibits a composite test made of an opal layer coating ~~the~~ internal part of the calcitic test. The thickness pattern of the opal layer, thick in the proloculus and thinning toward newer chambers, coupled to the identification of organelles involved in silica precipitation found for the first time in Foraminifera, ascribed to Silica Deposition Vesicles (SDVs), indicate that the *B. spissa* can silicify by itself. The deposition of opal appears to be discontinuous and to take place after ~~ward~~ calcite precipitation ~~phases~~, while occurring in different chambers at the same time. We ~~presume~~
500 ~~propose~~ that the opal layer may serve as a protection barrier against predators able to drill holes chemically or mechanically in the calcitic test~~s~~ of Foraminifera. However, others (non-exclusive) functions could exist and ~~are still need~~ to be investigated further. The presence of this ~~unnoticed until now overlooked~~ opal layer below the calcitic test ~~in of~~ the cosmopolitan *B. spissa* raises ~~the questions on the of silicification extend of silicification~~ in Foraminifera. The only other known silicifying species ~~is~~
505 ~~branching relatively far on phylogenetic trees and belongs to another foraminiferal class, branching relatively far on phylogenetic trees, belongs to another foraminiferal class, and p~~At the same time, preliminary observations on another *Bolivina* morphospecies exhibiting analogous structures below calcite could indicate that this trait may be more widespread than previously assumed. While the presence of this opal layer ~~below the calcitic test~~ may influence palaeoceanographic reconstruction using test composition, it may ~~also~~ lead to the development of new palaeoproxy(ies) based on this layer. ~~Finally,~~
510 ~~if silicification was found to be more widespread than previously known, it would probably make Foraminifera significant, so far overlooked, actors regarding the Si cycle at global scale.~~

a mis en forme : Police :Itaique

a mis en forme : Police :Itaique

a mis en forme : Police :Itaique

a mis en forme : Police :Itaique

a mis en forme : Police :Itaique

a mis en forme : Police :Itaique

Data availability

Raw data are available in the supplementary material attached to this manuscript.

Author contribution

515 **Julien Richirt**: conceptualisation, sampling, environmental SEM samples preparation and data acquisition, data interpretation, original draft writing. **Satoshi Okada**: sampling, cryo-SEM and FTIR samples preparation and data acquisition, data interpretation. **Yoshiyuki Ishitani**: sampling, data interpretation. **Katsuyuki Uematsu**: TEM samples preparation and data acquisition. **Akihiro Tame**: TEM samples preparation. **Kaya Oda**: Foraminifera picking, samples preparations. **Noriyuki Isobe**: FTIR data acquisition, data interpretation. **Toyoho Ishimura**: isotopic data acquisition and interpretation. **Masashi Tsuchiya**: data interpretation. **Hidetaka Nomaki**: conceptualisation, sampling, data interpretation. All co-authors participated in the writing, review, and editing process.

Competing interest

The authors declare that they have no competing interest.

Acknowledgments

525 We are grateful to the captains, crew members and onboard scientists of the research vessel R/V *Yokosuka* as well as the operation team of HOV *Shinkai 6500* for their help during samples collection. We would like to thank Takazo Shibuya (JAMSTEC) for his help regarding FTIR measurements, and Elena Golikova for generously providing us with literature otherwise difficult to access. This manuscript benefited of the valuable contributions of Lennart de Nooijer and an anonymous reviewer during the reviewing process. This work was supported by the Japan Society for the Promotion of Science (JSPS) funding P21729 and 21H01202.

References

Aitken, Z. H., Luo, S., Reynolds, S. N., Thaulow, C., and Greer, J. R.: Microstructure provides insights into evolutionary design and resilience of *Coscinodiscus* sp. frustule, Proceedings of the National Academy of Sciences, 113, 2017–2022, <https://doi.org/10.1073/pnas.1519790113>, 2016.

535 Alve, E. and Goldstein, S. T.: Dispersal, survival and delayed growth of benthic foraminiferal propagules, Journal of Sea Research, 63, 36–51, <https://doi.org/10.1016/j.seares.2009.09.003>, 2010.

Anderson, O. R.: Cytoplasmic origin and surface deposition of siliceous structures in Sarcodina, *Protoplasma*, 181, 61–77, <https://doi.org/10.1007/BF01666389>, 1994.

Arnold, A. J., d'Escrivan, F., and Parker, W. C.: Predation and avoidance responses in the foraminifera of the Galapagos hydrothermal mounds, *Journal of Foraminiferal Research*, 15, 38–42, <https://doi.org/10.2113/gsjfr.15.1.38>, 1985.

Bé, A. W. H. and Lott, L.: Shell Growth and Structure of Planktonic Foraminifera, *Science*, 145, 823–824, <https://doi.org/10.1126/science.145.3634.823>, 1964.

Bernhard, J. M., Buck, K. R., and Barry, J. P.: Monterey Bay cold-seep biota: Assemblages, abundance, and ultrastructure of living foraminifera, *Deep Sea Research Part I: Oceanographic Research Papers*, 48, 2233–2249, [https://doi.org/10.1016/S0967-0637\(01\)00017-6](https://doi.org/10.1016/S0967-0637(01)00017-6), 2001.

Bernhard, J. M., Goldstein, S. T., and Bowser, S. S.: An ectobiont-bearing foraminiferan, *Bolivina pacifica*, that inhabits microoxic pore waters: cell-biological and paleoceanographic insights, *Environmental Microbiology*, 12, 2107–2119, <https://doi.org/10.1111/j.1462-2920.2009.02073.x>, 2010.

Bernhard, J. M., Casciotti, K. L., McIlvin, M. R., Beaudoin, D. J., Visscher, P. T., and Edgcomb, V. P.: Potential importance of physiologically diverse benthic foraminifera in sedimentary nitrate storage and respiration, *Journal of Geophysical Research: Biogeosciences*, 117, <https://doi.org/10.1029/2012JG001949>, 2012.

Borrelli, C., Panieri, G., Dahl, T. M., and Neufeld, K.: Novel biomineralization strategy in calcareous foraminifera, *Scientific Reports*, 8, 10201, <https://doi.org/10.1038/s41598-018-28400-2>, 2018.

Brady, Expedition (1872-1876), C., Britain, G., Buchan, A., Huxley, T. H., Murray, J., Nares, G. S., Nares, G. S., Pelseneer, P., Thomson, C. W., Thomson, F. T., Thomson, F. T., and Challenger (Ship): Report on the scientific results of the voyage of H.M.S. Challenger during the years 1873-76 under the command of Captain George S. Nares and Captain Frank Tourle Thomson, R.N. Neill, Edinburgh, 858 pp., 1884.

Brümmer (auth.), F. and Müller (eds.), P. D. W. E. G.: Silicon Biomineralization: Biology — Biochemistry — Molecular Biology — Biotechnology, 1st ed., Springer-Verlag Berlin Heidelberg, 2003.

Bubenshchikova, N., Nürnberg, D., Lembke-Jene, L., and Pavlova, G.: Living benthic foraminifera of the Okhotsk Sea: Faunal composition, standing stocks and microhabitats, *Marine Micropaleontology*, 69, 314–333, <https://doi.org/10.1016/j.marmicro.2008.09.002>, 2008.

Burki, F., Roger, A. J., Brown, M. W., and Simpson, A. G. B.: The New Tree of Eukaryotes, *Trends in Ecology & Evolution*, 35, 43–55, <https://doi.org/10.1016/j.tree.2019.08.008>, 2020.

Burmistrova, I. I.: K stratigrafii glubokovodnykh osadkov vostochnoy chasti Indiyaskogo Okeana po bentosnym foraminiferam [On the stratigraphy of deep sea deposits in the eastern part of the Indian Ocean, based on benthic foraminifera], in *Morskaya Mikropaleontologiya*, Moscow: Akademiya Nauk SSSR, Okeanograficheskaya Komissiya, 163–170, 1978.

Cedhagen, T.: Taxonomy and biology of *Hyrrokin sarcophaga* gen. et sp. n., a parasitic foraminiferan (Rosalinidae), *Sarsia*, 79, 65–82, <https://doi.org/10.1080/00364827.1994.10413549>, 1994.

a mis en forme : Police par défaut

a mis en forme : Justifié, Interligne : 1,5 ligne

a mis en forme : Police par défaut

a mis en forme : Police par défaut

- 570 Cesbron, F., Geslin, E., Jorissen, F. J., Delgard, M. L., Charrieau, L., Deflandre, B., Jézéquel, D., Anschutz, P., and Metzger, E.: Vertical distribution and respiration rates of benthic foraminifera: Contribution to aerobic remineralization in intertidal mudflats covered by *Zostera noltei* meadows, *Estuarine, Coastal and Shelf Science*, 179, 23–38, <https://doi.org/10.1016/j.ecss.2015.12.005>, 2016.
- Chen, C. T. A., Feely, R. A., and Gendron, J. F.: Lysocline, Calcium Carbonate Compensation Depth, and Calcareous Sediments in the North Pacific Ocean, 1988.
- 575 Culver, S. J.: Early Cambrian Foraminifera from West Africa, *Science*, 254, 689–691, <https://doi.org/10.1126/science.254.5032.689>, 1991.
- Culver, S. J. and Lipps, J. H.: Predation on and by Foraminifera, in: *Predator—Prey Interactions in the Fossil Record*, edited by: Kelley, P. H., Kowalewski, M., and Hansen, T. A., Springer US, Boston, MA, 7–32, [https://doi.org/10.1007/978-1-4615-](https://doi.org/10.1007/978-1-4615-0161-9_2)
- 580 0161-9_2, 2003.
- Cushman, J. A.: Some Pliocene *Bolivinas* from California, *Contributions from the Cushman laboratory for foraminiferal research*, 2, 40–47, 1926.
- Darling, K. F., Thomas, E., Kasemann, S. A., Seears, H. A., Smart, C. W., and Wade, C. M.: Surviving mass extinction by bridging the benthic/planktic divide, *Proceedings of the National Academy of Sciences*, 106, 12629–12633, <https://doi.org/10.1073/pnas.0902827106>, 2009.
- 585 De La Rocha, C. L.: Opal-based isotopic proxies of paleoenvironmental conditions, *Global Biogeochemical Cycles*, 20, <https://doi.org/10.1029/2005GB002664>, 2006.
- Donald, H. K., Foster, G. L., Fröhberg, N., Swann, G. E. A., Poulton, A. J., Moore, C. M., and Humphreys, M. P.: The pH dependency of the boron isotopic composition of diatom opal (*Thalassiosira weissflogii*), *Biogeosciences*, 17, 2825–2837, <https://doi.org/10.5194/bg-17-2825-2020>, 2020.
- 590 Drum, R. W. and Pankratz, H. S.: Post mitotic fine structure of *Gomphonema parvulum*, *Journal of Ultrastructure Research*, 10, 217–223, [https://doi.org/10.1016/s0022-5320\(64\)80006-x](https://doi.org/10.1016/s0022-5320(64)80006-x), 1964.
- Dubicka, Z.: Chamber arrangement versus wall structure in the high-rank phylogenetic classification of Foraminifera, *Acta Palaeontologica Polonica*, 64, <https://doi.org/10.4202/app.00564.2018>, 2019.
- 595 Echols, R. J.: Distribution of Foraminifera in Sediments of the Scotia Sea Area, Antarctic Waters, in: *Antarctic Oceanology I*, American Geophysical Union (AGU), 93–168, <https://doi.org/10.1029/AR015p0093>, 1971.
- Ehrlich, H. L., Newman, D. K., and Kappler, A. (Eds.): *Ehrlich's Geomicrobiology*, 6th edition., CRC Press, 656 pp., 2016.
- Foissner, W., Weissenbacher, B., Krautgartner, W.-D., and Lütz-Meindl, U.: A Cover of Glass: First Report of Biomineralized Silicon in a Ciliate, *Maryna umbrellata* (Ciliophora: Colpodea), *Journal of Eukaryotic Microbiology*, 56, 519–530, <https://doi.org/10.1111/j.1550-7408.2009.00431.x>, 2009.
- 600 Fontanier, C., Duros, P., Toyofuku, T., Oguri, K., Koho, K. A., Buscail, R., Gremare, A., Radakovitch, O., Deflandre, B., De Nooijer, L. J., Bichon, S., Goubet, S., Ivanovsky, A., Chabaud, G., Menniti, C., Reichart, G.-J., and Kitazato, H.: living

- (stained) deep-sea foraminifera off Hachinohe (NE Japan, western Pacific): environmental interplay in oxygen-depleted ecosystems, *The Journal of Foraminiferal Research*, 44, 281–299, <https://doi.org/10.2113/gsjfr.44.3.281>, 2014.
- 605 Garrone, R., Simpson, T. L., and Pottu-Boumendil, J.: Ultrastructure and Deposition of Silica in Sponges, in: *Silicon and Siliceous Structures in Biological Systems*, edited by: Simpson, T. L. and Volcani, B. E., Springer, New York, NY, 495–525, https://doi.org/10.1007/978-1-4612-5944-2_17, 1981.
- Glock, N., Eisenhauer, A., Milker, Y., Liebetrau, V., Schönfeld, J., Mallon, J., Sommer, S., and Hensen, C.: Environmental Influences on the Pore Density of *Bolivina Spissa* (Cushman), *Journal of Foraminiferal Research*, 41, 22–32, 610 <https://doi.org/10.2113/gsjfr.41.1.22>, 2011.
- Glock, N., Eisenhauer, A., Liebetrau, V., Wiedenbeck, M., Hensen, C., and Nehrke, G.: EMP and SIMS studies on Mn/Ca and Fe/Ca systematics in benthic foraminifera from the Peruvian OMZ: a contribution to the identification of potential redox proxies and the impact of cleaning protocols, *Biogeosciences*, 9, 341–359, <https://doi.org/10.5194/bg-9-341-2012>, 2012.
- Glock, N., Roy, A.-S., Romero, D., Wein, T., Weissenbach, J., Revsbech, N. P., Høglund, S., Clemens, D., Sommer, S., and 615 Dagan, T.: Metabolic preference of nitrate over oxygen as an electron acceptor in foraminifera from the Peruvian oxygen minimum zone, [PNAS Proceedings of the National Academy of Sciences](https://doi.org/10.1073/pnas.1813887116), 116, 2860–2865, <https://doi.org/10.1073/pnas.1813887116>, 2019.
- Glud, R. N., Thamdrup, B., Stahl, H., Wenzhoefer, F., Glud, A., Nomaki, H., Oguri, K., Revsbech, N. P., and Kitazato, H.: Nitrogen cycling in a deep ocean margin sediment (Sagami Bay, Japan), *Limnology and Oceanography*, 54, 723–734, 620 <https://doi.org/10.4319/lo.2009.54.3.0723>, 2009.
- Goldstein, S. T. and Corliss, B. H.: Deposit feeding in selected deep-sea and shallow-water benthic foraminifera, *Deep Sea Research Part I: Oceanographic Research Papers*, 41, 229–241, [https://doi.org/10.1016/0967-0637\(94\)90001-9](https://doi.org/10.1016/0967-0637(94)90001-9), 1994.
- Gooday, A. J., Levin, L. A., Linke, P., and Heeger, T.: The Role of Benthic Foraminifera in Deep-Sea Food Webs and Carbon Cycling, in: *Deep-Sea Food Chains and the Global Carbon Cycle*, edited by: Rowe, G. T. and Pariente, V., Springer 625 Netherlands, Dordrecht, 63–91, https://doi.org/10.1007/978-94-011-2452-2_5, 1992.
- Gooday, A. J., Nomaki, H., and Kitazato, H.: Modern deep-sea benthic foraminifera: a brief review of their morphology-based biodiversity and trophic diversity, *Geological Society, London, Special Publications*, 303, 97–119, <https://doi.org/10.1144/SP303.8>, 2008.
- Greenwood, N. N. and Earnshaw, A.: *Chemistry of the Elements*, Elsevier, 1365 pp., 1997.
- 630 Groussin, M., Pawlowski, J., and Yang, Z.: Bayesian relaxed clock estimation of divergence times in foraminifera, *Molecular Phylogenetics and Evolution*, 61, 157–166, <https://doi.org/10.1016/j.ympev.2011.06.008>, 2011.
- Gupta, B. K. S.: *Modern Foraminifera*, Springer Science & Business Media, 368 pp., 2003.
- Hallock, P. and Talge, H.: A Predatory Foraminifer, *Floresina amphiphaga*, n. sp., from the Florida Keys, *Journal of Foraminiferal Research*, 24, 210–213, <https://doi.org/10.2113/gsjfr.24.4.210>, 1994.

- 635 Hamm, C. E., Merkel, R., Springer, O., Jurkojc, P., Maier, C., Prechtel, K., and Smetacek, V.: Architecture and material properties of diatom shells provide effective mechanical protection, *Nature*, 421, 841–843, <https://doi.org/10.1038/nature01416>, 2003.
- Hansen, H. J.: Shell construction in modern calcareous Foraminifera, in: *Modern Foraminifera*, edited by: Sen Gupta, B. K., Springer Netherlands, Dordrecht, 57–70, https://doi.org/10.1007/0-306-48104-9_4, 2003.
- 640 Heinz, P., Sommer, S., Pfannkuche, O., and Hemleben, C.: Living benthic foraminifera in sediments influenced by gas hydrates at the Cascadia convergent margin, NE Pacific, *Marine Ecology Progress Series*, 304, 77–89, <https://doi.org/10.3354/meps304077>, 2005.
- Hendry, K. R., Georg, R. B., Rickaby, R. E. M., Robinson, L. F., and Halliday, A. N.: Deep ocean nutrients during the Last Glacial Maximum deduced from sponge silicon isotopic compositions, *Earth and Planetary Science Letters*, 292, 290–300, <https://doi.org/10.1016/j.epsl.2010.02.005>, 2010.
- 645 Hendry, K. R., Marron, A. O., Vincent, F., Conley, D. J., Gehlen, M., Ibarbalz, F. M., Quéguiner, B., and Bowler, C.: Competition between Silicifiers and Non-silicifiers in the Past and Present Ocean and Its Evolutionary Impacts, *Frontiers in Marine Science*, 5, <https://doi.org/10.3389/fmars.2018.00022>, 2018.
- Herbert, D. G.: Foraminiferivory in a *Puncturella* (Gastropoda: Fissurellidae), *Journal of Molluscan Studies*, 57, 127–129, <https://doi.org/10.1093/mollus/57.1.127>, 1991.
- 650 Hickman, C. S. and Lipps, J. H.: Foraminiferivory; selective ingestion of foraminifera and test alterations produced by the neogastropod *Olivella*, *Journal of Foraminiferal Research*, 13, 108–114, <https://doi.org/10.2113/gsjfr.13.2.108>, 1983.
- Holzmann, M. and Pawlowski, J.: An updated classification of rotaliid foraminifera based on ribosomal DNA phylogeny, *Marine Micropaleontology*, 132, 18–34, <https://doi.org/10.1016/j.marmicro.2017.04.002>, 2017.
- 655 Ishimura, T., Tsunogai, U., and Gamo, T.: Stable carbon and oxygen isotopic determination of sub-microgram quantities of CaCO₃ to analyze individual foraminiferal shells, *Rapid Communications in Mass Spectrometry*, 18, 2883–2888, <https://doi.org/10.1002/rcm.1701>, 2004.
- Ishimura, T., Tsunogai, U., and Nakagawa, F.: Grain-scale heterogeneities in the stable carbon and oxygen isotopic compositions of the international standard calcite materials (NBS 19, NBS 18, IAEA-CO-1, and IAEA-CO-8), *Rapid Communications in Mass Spectrometry*, 22, 1925–1932, <https://doi.org/10.1002/rcm.3571>, 2008.
- 660 Ishimura, T., Tsunogai, U., Hasegawa, S., Nakagawa, F., Oi, T., Kitazato, H., Suga, H., and Toyofuku, T.: Variation in stable carbon and oxygen isotopes of individual benthic foraminifera: tracers for quantifying the magnitude of isotopic disequilibrium, *Biogeosciences*, 9, 4353–4367, <https://doi.org/10.5194/bg-9-4353-2012>, 2012.
- Jauffrais, T., LeKieffre, C., Koho, K. A., Tsuchiya, M., Schweizer, M., Bernhard, J. M., Meibom, A., and Geslin, E.: Ultrastructure and distribution of kleptoplasts in benthic foraminifera from shallow-water (photic) habitats, *Marine Micropaleontology*, 138, 46–62, <https://doi.org/10.1016/j.marmicro.2017.10.003>, 2018.
- 665 Jones, R. W.: *Foraminifera and their Applications*, Cambridge University Press, 407 pp., 2013.

a mis en forme : Police par défaut

- Katz, M. E., Cramer, B. S., Franzese, A., Hönisch, B., Miller, K. G., Rosenthal, Y., and Wright, J. D.: Traditional and emerging geochemical proxies in foraminifera, *Journal of Foraminiferal Research*, 40, 165–192, <https://doi.org/10.2113/gsjfr.40.2.165>, 2010.
- 670 [Kaźmierczak, J., Ittekkot, V., and Degens, E. T.: Biocalcification through time: environmental challenge and cellular response, *Paläont. Z.*, 59, 15–33, <https://doi.org/10.1007/BF02985996>, 1985.](#)
- Keating-Bitonti, C. R. and Payne, J. L.: Ecophenotypic responses of benthic foraminifera to oxygen availability along an oxygen gradient in the California Borderland, *Marine Ecology*, 38, e12430, <https://doi.org/10.1111/maec.12430>, 2017.
- 675 Kitazato, H., Shirayama, Y., Nakatsuka, T., Fujiwara, S., Shimanaga, M., Kato, Y., Okada, Y., Kanda, J., Yamaoka, A., Masuzawa, T., and Suzuki, K.: Seasonal phytodetritus deposition and responses of bathyal benthic foraminiferal populations in Sagami Bay, Japan: preliminary results from “Project Sagami 1996–1999,” *Marine Micropaleontology*, 40, 135–149, [https://doi.org/10.1016/S0377-8398\(00\)00036-0](https://doi.org/10.1016/S0377-8398(00)00036-0), 2000.
- Knoll, A. H. and Kotrc, B.: Protistan Skeletons: A Geologic History of Evolution and Constraint, in: *Evolution of Lightweight Structures: Analyses and Technical Applications*, edited by: Hamm, C., Springer Netherlands, Dordrecht, 1–16, https://doi.org/10.1007/978-94-017-9398-8_1, 2015.
- 680 Koho, K. A., de Nooijer, L. J., Fontanier, C., Toyofuku, T., Oguri, K., Kitazato, H., and Reichart, G.-J.: Benthic foraminiferal Mn / Ca ratios reflect microhabitat preferences, *Biogeosciences*, 14, 3067–3082, <https://doi.org/10.5194/bg-14-3067-2017>, 2017.
- 685 Krabberød, A. K., Orr, R. J. S., Bråte, J., Kristensen, T., Bjørklund, K. R., and Shalchian-Tabrizi, K.: Single Cell Transcriptomics, Mega-Phylogeny, and the Genetic Basis of Morphological Innovations in Rhizaria, *Molecular Biology and Evolution*, 34, 1557–1573, <https://doi.org/10.1093/molbev/msx075>, 2017.
- Kucera, M., Silve, L., Weiner, A. K. M., Darling, K., Lübben, B., Holzmann, M., Pawlowski, J., Schönfeld, J., and Morard, R.: Caught in the act: anatomy of an ongoing benthic–planktonic transition in a marine protist, *Journal of Plankton Research*, 690 39, 436–449, <https://doi.org/10.1093/plankt/fbx018>, 2017.
- Langer, M. R.: Assessing the Contribution of Foraminiferan Protists to Global Ocean Carbonate Production¹, *Journal of Eukaryotic Microbiology*, 55, 163–169, <https://doi.org/10.1111/j.1550-7408.2008.00321.x>, 2008.
- Larkin, P.: *Infrared and Raman Spectroscopy: Principles and Spectral Interpretation*, Elsevier, 239 pp., 2011.
- 695 LeKieffre, C., Bernhard, J. M., Mabilieu, G., Filipsson, H. L., Meibom, A., and Geslin, E.: An overview of cellular ultrastructure in benthic foraminifera: New observations of rotalid species in the context of existing literature, *Marine Micropaleontology*, 138, 12–32, <https://doi.org/10.1016/j.marmicro.2017.10.005>, 2018.
- Llopis Monferrer, N., Boltovskoy, D., Tréguer, P., Sandin, M. M., Not, F., and Leynaert, A.: Estimating Biogenic Silica Production of Rhizaria in the Global Ocean, *Global Biogeochemical Cycles*, 34, e2019GB006286, <https://doi.org/10.1029/2019GB006286>, 2020.
- 700 Lowenstam, H. A.: Opal Precipitation by Marine Gastropods (Mollusca), *Science*, 171, 487–490, <https://doi.org/10.1126/science.171.3970.487>, 1971.

a mis en forme : Justifié, Interligne : 1,5 ligne

a mis en forme : Police par défaut

- Marron, A. O., Ratcliffe, S., Wheeler, G. L., Goldstein, R. E., King, N., Not, F., de Vargas, C., and Richter, D. J.: The Evolution of Silicon Transport in Eukaryotes, *Molecular Biology and Evolution*, 33, 3226–3248, <https://doi.org/10.1093/molbev/msw209>, 2016.
- 705 Marszalek, D. S., Wright, R. C., and Hay, W. W.: Function of the Test in Foraminifera, *Gulf Coast. Assoc. Geological Societies Trans.*, 19, 341–352, 1969.
- Mayerhöfer, T. G., Pahlow, S., Hübner, U., and Popp, J.: CaF₂: An Ideal Substrate Material for Infrared Spectroscopy?, *Anal-ytical Chemistry*, 92, 9024–9031, <https://doi.org/10.1021/acs.analchem.0c01158>, 2020.
- Moodley, L., Boschker, H. T. S., Middelburg, J. J., Pel, R., Herman, P. M. J., Deckere, E. de, and Heip, C. H. R.: Ecological significance of benthic foraminifera: ¹³C labelling experiments, *Marine Ecology Progress Series*, 202, 289–295, <https://doi.org/10.3354/meps202289>, 2000.
- 710 Mukherjee, S.: *Applied Mineralogy: Applications in Industry and Environment*, Springer Science & Business Media, 585 pp., 2012.
- Murray, J. W.: *Ecology and Applications of Benthic Foraminifera*, Cambridge University Press, Cambridge, <https://doi.org/10.1017/CBO9780511535529>, 2006.
- 715 Murray, J. W.: Biodiversity of living benthic foraminifera: How many species are there?, *Marine Micropaleontology*, 64, 163–176, <https://doi.org/10.1016/j.marmicro.2007.04.002>, 2007.
- Nagai, Y., Uematsu, K., Chen, C., Wani, R., Tyszka, J., and Toyofuku, T.: Weaving of biomineralization framework in rotaliid foraminifera: implications for paleoceanographic proxies, *Biogeosciences*, 15, 6773–6789, [https://doi.org/10.5194/bg-15-](https://doi.org/10.5194/bg-15-6773-2018)
- 720 [6773-2018](https://doi.org/10.5194/bg-15-6773-2018), 2018.
- [Nardelli, M. P., Barras, C., Metzger, E., Mouret, A., Filipsson, H. L., Jorissen, F., and Geslin, E.: Experimental evidence for foraminiferal calcification under anoxia, *Biogeosciences*, 11, 4029–4038, <https://doi.org/10.5194/bg-11-4029-2014>, 2014.](https://doi.org/10.5194/bg-11-4029-2014)
- Nielsen, K. S. S.: Foraminiferivory revisited: a preliminary investigation of holes in foraminifera, *Bulletin of the Geological Society of Denmark*, 45, 139–142, 1999.
- 725 Nomaki, H., Heinz, P., Nakatsuka, T., Shimanaga, M., Ohkouchi, N., Ogawa, N. O., Kogure, K., Ikemoto, E., and Kitazato, H.: Different ingestion patterns of ¹³C-labeled bacteria and algae by deep-sea benthic foraminifera, *Marine Ecology Progress Series*, 310, 95–108, <https://doi.org/10.3354/meps310095>, 2006.
- Nomaki, H., Ogawa, N. O., Ohkouchi, N., Suga, H., Toyofuku, T., Shimanaga, M., Nakatsuka, T., and Kitazato, H.: Benthic foraminifera as trophic links between phytodetritus and benthic metazoans: carbon and nitrogen isotopic evidence, *Marine Ecology Progress Series*, 357, 153–164, <https://doi.org/10.3354/meps07309>, 2008.
- 730 de Nooijer, L. J., Spero, H. J., Erez, J., Bijma, J., and Reichart, G. J.: Biomineralization in perforate foraminifera, *Earth-Science Reviews*, 135, 48–58, <https://doi.org/10.1016/j.earscirev.2014.03.013>, 2014.
- de Nooijer, L. J., Pacho Sampedro, L., Jorissen, F. J., Pawlowski, J., Rosenthal, Y., Dissard, D., and Reichart, G. J.: 500 million years of foraminiferal calcification, *Earth-Science Reviews*, 243, 104484, <https://doi.org/10.1016/j.earscirev.2023.104484>, 2023.

Okada, S., Richirt, J., Tame, A., and Nomaki, H.: Rapid Freezing and Cryo-SEM-EDS Imaging of Foraminifera (Unicellular Eukaryotes) Using a Conductive Viscous Cryogenic Glue. *Microscopy and Microanalysis*, 30, 359–367, <https://doi.org/10.1093/mam/ozae026>, 2024.

Orsi, W. D., Morard, R., Vuillemin, A., Eitel, M., Wörheide, G., Milucka, J., and Kucera, M.: Anaerobic metabolism of Foraminifera thriving below the seafloor. *The ISME Journal*, 14, 2580–2594, <https://doi.org/10.1038/s41396-020-0708-1>, 2020.

Parker, J. H.: Ultrastructure of the Test Wall in Modern Porcelaneous Foraminifera: Implications For the Classification of the Miliolida. *Journal of Foraminiferal Research*, 47, 136–174, <https://doi.org/10.2113/gsjfr.47.2.136>, 2017.

Pawlowski, J., Holzmann, M., and Tyszka, J.: New supraordinal classification of Foraminifera: Molecules meet morphology. *Marine Micropaleontology*, 100, 1–10, <https://doi.org/10.1016/j.marmicro.2013.04.002>, 2013.

Piña-Ochoa, E., Høgslund, S., Geslin, E., Cedhagen, T., Revsbech, N. P., Nielsen, L. P., Schweizer, M., Jorissen, F., Rysgaard, S., and Risgaard-Petersen, N.: Widespread occurrence of nitrate storage and denitrification among Foraminifera and Gromiida. *Proceedings of the National Academy of SciencesPNAS*, 107, 1148–1153, <https://doi.org/10.1073/pnas.0908440107>, 2010.

Reka, A. A., Pavlovski, B., Fazlija, E., Berisha, A., Pacarizi, M., Daghmehchi, M., Sacalis, C., Jovanovski, G., Makreski, P., and Oral, A.: Diatomaceous Earth: Characterization, thermal modification, and application. *Open Chemistry*, 19, 451–461, <https://doi.org/10.1515/chem-2020-0049>, 2021.

Resig, J. M., Lowenstam, H. A., Echols, R. J., and Weiner, S.: An extant opaline foraminifer: test ultrastructure, mineralogy, and taxonomy, in: *Studies in Marine Micropaleontology and Paleocology: A Memorial Volume to Orville L. Bandy*, vol. 19, edited by: Sliter, W. V., Cushman Foundation for Foraminiferal Research, 205–2140, 1980.

Schindelin, J., Arganda-Carreras, I., Frise, E., Kaynig, V., Longair, M., Pietzsch, T., Preibisch, S., Rueden, C., Saalfeld, S., Schmid, B., Tinevez, J.-Y., White, D. J., Hartenstein, V., Eliceiri, K., Tomancak, P., and Cardona, A.: Fiji: an open-source platform for biological-image analysis. *Nat Methods*, 9, 676–682, <https://doi.org/10.1038/nmeth.2019>, 2012.

Sierra, R., Mauffrey, F., Cruz, J., Holzmann, M., Gooday, A. J., Maurer-Alcalá, X., Thakur, R., Greco, M., Weiner, A. K. M., Katz, L. A., and Pawlowski, J.: Taxon-rich transcriptomics supports higher-level phylogeny and major evolutionary trends in Foraminifera. *Molecular Phylogenetics and Evolution*, 174, 107546, <https://doi.org/10.1016/j.ympev.2022.107546>, 2022.

Simkiss, K.: Biomineralization and detoxification. *Calc. Tis Res.*, 24, 199–200, <https://doi.org/10.1007/BF02223316>, 1977.

Sliter, W. V.: Predation on benthic foraminifers. *Journal of Foraminiferal Research*, 1, 20–28, <https://doi.org/10.2113/gsjfr.1.1.20>, 1971.

Socrates, G.: *Infrared and Raman Characteristic Group Frequencies: Tables and Charts*, John Wiley & Sons, 386 pp., 2004.

Stefano, L. D., Stefano, M. D., Rea, I., Moretti, L., Bismuto, A., Maddalena, P., and Rendina, I.: Optical characterisation of biological nano-porous silica structures, in: *Nanophotonic Materials and Systems II*, Nanophotonic Materials and Systems II, 106–110, <https://doi.org/10.1117/12.619450>, 2005.

a mis en forme : Justifié, Interligne : 1,5 ligne

a mis en forme : Police par défaut

a mis en forme : Français (France)

a mis en forme : Police par défaut, Français (France)

a mis en forme : Français (France)

a mis en forme : Justifié, Interligne : 1,5 ligne

Code de champ modifié

- Toyofuku, T., Matsuo, M. Y., Nooijer, L. J. de, Nagai, Y., Kawada, S., Fujita, K., Reichart, G.-J., Nomaki, H., Tsuchiya, M., Sakaguchi, H., and Kitazato, H.: Proton pumping accompanies calcification in foraminifera, *Nature Communications*, 8, ~~141456~~, <https://doi.org/10.1038/ncomms14145>, 2017.
- ~~Tréguer, P. J., Sutton, J. N., Brzezinski, M., Charette, M. A., Devries, T., Dutkiewicz, S., Ehlert, C., Hawkings, J., Leynaert, A., Liu, S. M., Llopis Monferrer, N., López-Acosta, M., Maldonado, M., Rahman, S., Ran, L., and Rouxel, O.: Reviews and syntheses: The biogeochemical cycle of silicon in the modern ocean, *Biogeosciences*, 18, 1269–1289, <https://doi.org/10.5194/bg-18-1269-2021>, 2021.~~
- 775 Trower, E. J., Strauss, J. V., Sperling, E. A., and Fischer, W. W.: Isotopic analyses of Ordovician–Silurian siliceous skeletons indicate silica-depleted Paleozoic oceans, *Geobiology*, 19, 460–472, <https://doi.org/10.1111/gbi.12449>, 2021.
- Ujiié, Y., Ishitani, Y., Nagai, Y., Takaki, Y., Toyofuku, T., and Ishii, S.: Unique evolution of foraminiferal calcification to survive global changes, *Science Advances*, 9, eadd3584, <https://doi.org/10.1126/sciadv.add3584>, 2023.
- Wetmore, K. L.: Correlations between test strength, morphology and habitat in some benthic foraminifera from the coast of Washington, *Journal of Foraminiferal Research*, 17, 1–13, <https://doi.org/10.2113/gsjfr.17.1.1>, 1987.
- 780 Woehle, C., Roy, A.-S., Glock, N., Michels, J., Wein, T., Weissenbach, J., Romero, D., Hiebenthal, C., Gorb, S. N., Schönfeld, J., and Dagan, T.: Denitrification in foraminifera has an ancient origin and is complemented by associated bacteria, *Proceedings of the National Academy of Sciences*, 119, e2200198119, <https://doi.org/10.1073/pnas.2200198119>, 2022.
- Xu, Z., Liu, S., Xiang, R., and Song, G.: Live benthic foraminifera in the Yellow Sea and the East China Sea: vertical distribution, nitrate storage, and potential denitrification, *Marine Ecology Progress Series*, 571, 65–81, <https://doi.org/10.3354/meps12135>, 2017.
- 785 Zachos, J., Pagani, M., Sloan, L., Thomas, E., and Billups, K.: Trends, Rhythms, and Aberrations in Global Climate 65 Ma to Present, *Science*, 292, 686–693, <https://doi.org/10.1126/science.1059412>, 2001.